Dynamics and distribution of ARFB1b and ARFB1c GTPases in *N. tabacum* plant cells

Dissertation

zur

Erlangung des Doktorgrades (Dr. rer. nat.)

der

Mathematisch-Naturwissenschaftlichen Fakultät

der

Rheinischen Friedrich-Wilhelms-Universität Bonn

vorgelegt von

Luciana Renna

aus

Milano, ITALY

Bonn, 2009

Angefertigt mit Genehmigung der Mathematisch-Naturwissenschaftlichen Fakultät der Rheinischen Friedrich-Wilhelms-Universität Bonn

1. Referent: Prof. Dr. Dieter Volkmann

2. Referent: Prof. Dr. Diedrik Menzel

Tag der Promotion: 23 July 2009

Diese Dissertation ist auf dem Hochschulschriftenserver der ULB Bonn http://hss.ulb.unibonn.de/diss_online elektronisch publiziert.

Erscheinungsjahr: 2009

SUMMARY

Eukaryotic cells are characterized by a complex of endomembranes. The main organelles of this complex are the endoplasmic reticulum, the Golgi apparatus, the *trans*-Golgi network, the vacuoles, and the plasma membrane. In cells the endomembrane system identity and interconnection is preserved by an active intracellular trafficking mediated by vesicles, which shuttle cargo molecules such as proteins, polysaccharides, and lipids between these organelles. During the intracellular trafficking, vesicle fusion and budding is driven by the assembly and disassembly of the coat proteins from the membrane. In turn, assembly and disassembly of coat proteins are regulated by other proteins called ADP-Ribosylation Factors (ARFs), a subfamily of the Ras GTP-binding proteins superfamily, which switching from the inactive form (ARFGDP) to the active form (ARFGTP) regulates the assembly and the disassembly of the coat proteins.
The conversion between the inactive and active form is mediated by Guanine Exchange Factors (GEFs), while the active form is converted into the inactivated form by GTPase Activating Proteins (GAPs). ARFGTP peripherally associates with the organelle membrane and starts to recruits coat proteins from the cytosol. These coat proteins drive the membrane budding, capturing at the same time specific cargo molecules. After the hydrolysis of the ARFGTP form into ARFGDP, which is released into the cytosol, the coat component proteins detach from the membrane. In this way vesicles can dock and fuse with the target membrane.
In yeast and mammalian cells an active role of ARFs in the endocytic pathway has been demonstrated by creating mutants of this protein and seeing a blockage of this pathway. Vesicle trafficking in plants has functions similar to those in animal and yeast. In addition, it is necessary for non-cellulose polysaccharides delivery to the plant cell wall. All the regulatory roles in which ARFs are involved: membrane traffic, lipid metabolism, organelle morphology and cellular signalling, have been difficult to dissect due to the complexity of the ARF family.
In *A. thaliana* 12 ARFs have been identified, but for most of them the functionality is completely unknown. Moreover, no role has yet been identified for any of them, in the endocytic pathway.
Bioinformatics analysis of ARF proteins: In this work, the selection of possible ARFs involved in the endocytic pathways has been done making a BlastP of *A. thaliana* ARFs sub-family, considering the presence of the specific motif MxxE, which enables ARF1 to localize to the early Golgi apparatus. Recent evidence has shown that the motifs MxxE match the motif ILTD in ARFB1a (the homologue of the human ARF6). For this protein, the motif ILTD enables ARFB1a to localize at the plasma membrane and to take part in the endocytic pathway. Using BlastP other two ARFs were identified: ARFB1b and ARFB1c with a similar motif IIKD and IIRD and with an additional DPF motif important for AP2 interaction in human. All these characteristics suggest these two proteins as ideal candidate for having crucial function in the endocytotic machinery.
ArfB1b and ArfB1c localization: For each of these proteins GFP/YFP fusions were created. The constructs so obtained were used to localize them in living epidermis cells of *Nicotiana tabacum* by confocal microscopy. The novel proteins plus ARF1 and ARFB1a (used as controls) were coexpressed with ERD2, a marker for the Golgi apparatus, with the SNARE SYP61, a marker for the Trans Golgi network, with the FYVE domain construct, marker for the early and late endosomes and with the two RAB GTPases RHAI

and ARA7 markers of the PVC (pre-vacuolar compartment) and the early and late endosomes respectively. The experiment of colocalization with all these specific markers localizes both ARFB1b and ARFB1c at the TGN (Trans Golgi network) and for ARFB1c a partial co-localization with FYVE domain construct and ARA7 was observed. Furthermore cross-colocalization between ARF1, ARFB1a, ARFB1b and ARFB1c, shows that these proteins overlap in their colocalization on the *trans* Golgi apparatus.
Kinetic analysis: To evaluate the cellular dynamics of the ARF proteins used in this work, a study of the kinetics of these proteins was performed using FRAP (Fluorescence Recovery After Photobleaching) analysis.
A different kinetic was found for each of the examined proteins.
ARF1 wt has a relatively slow half maximal recovery time equal to 10.9± 1.5 s (seconds), compared to the wt form ARF1GTP which has a recovery time of 19± 3.0 s, ARFB1awt recovers in 16± 1.4 s, and ARFB1aGTP which recovers in 33.6± 3.2 s. ARFB1bwt recovers in 12.2± 2.6 s and the GTP bound form in 16.3± 2.8 s; for ARFB1c the half maximal recovery time is 12.6± 1.5 s, while its GTP form recycles in 24.3± 4.2 s.
The fluorescence recovery time of some ARFGTPs at the Golgi or non Golgi apparatus membrane suggested that the GTP mutants' ability recycling is not entirely abolished, the kinetic studies also show that ARFs are highly mobile and that ARFs GTP bound form diffuses more slowly compared to ARFs in wt form. Furthermore, the different recovery times suggest a distinct role in the secretory pathway. The higher speed of recovery for ARF1 and ARF1GTP compared to the ARFB1a, which localizes to the plasma membrane, suggests that this protein is important to maintain equilibrium between the anterograde and the retrograde pathways. Similar observations for the ARFB1b and ARFB1c, suggest that they may maintain equilibrium during the traffic at the TGN, which involves endosomes, plasma membrane and PVC.
ARF1, ARFB1a, ARFB1b and ARFB1c have different impacts on protein secretion in *N. tabacum* transformed protoplast: To evaluate the impact of these ARFs on the protein secretion the wt forms of the proteins were co-transformed with the secretory marker SecRGUS. The results obtained were compared with another experiment in which the impact on the secretion of the GDP mutant form was evaluated. The secretion test shows that ARF1GDP inhibits proteins secretion. ARFB1bwt stimulates secretion, compared to ARF1wt and ARFB1a. In contrast ARFB1bGDP hampers secretion more than ARF1GDP. ARFB1c has more or less no effect on the secretion in the wt form, while in the GDP form it seems to have less inhibitory effect than ARFB1bGDP. Taking together these results suggest that ARFB1b and ARFB1c have a remarkable influence on secretion processes. Furthermore it is hypothesized that they are involved in two different secretory pathways, ARFB1b directed to the plasma membrane and ARFB1c to the endosomes. These results show that blocking the pathway in which one of the proteins is involved, it is stimulated a parallel pathway probably to maintain stability and structure of the endomembrane system, in order to protect the equilibrium and functionality of the cell.

TABLE OF CONTENTS

LIST OF FIGURES

LIST OF TABLES

LIST OF ABBREVIATIONS

ARF	ADP Ribosilation Factor
bp	base pair
cDNA	complementary DNA
CFP	Cyan Fluorescent Protein
COPI	Coat Protein complex I
COPII	Coat Protein complex II
DNA	Deoxyribonucleic Acid
dNTPs	deoxyribonucleotide triphosphates
EDTA	Ethylenediaminetetraacetic acid
ER	Endoplasmic Reticulum
ERD2	Endoplasmic Reticulum Retention Defective 2
GAP	GTPase Activating Protein
GDP	Guanosine diphosphate
GEF	Guanine nucleotide Exchange Factor
GFP	Green Fluorescent Protein
GTP	Guanosine triphosphates
Kb	Kilobase
LB	Luria Bertani
LV	Lytic Vacuole
MES	2-(N-morpholino) ethane-sulfonic acid
NE	Nuclear Envelope

PBS	Phosphate Buffered Saline
PCR	Polymerase Chain Reaction
PVC	Pre-Vacuolar Compartment
Rab	Ras-like protein in brain
RER	Rough Endoplasmic Reticulum
SER	Smooth Endoplasmic Reticulum
SDS	Sodium Dodecyl Sulphate
SH3	Src Homology-3
SecRGUS	Secreted Rat β-glucuronidase
SNAREs	Soluble N-ethyl maleimide sensitive factor attachment protein receptors
TAE	Tris-acetate-EDTA
TEMED	Tetra-methyl-ethylene-diamine
TFBI	Transformation Buffer I
TFBII	Transformation Buffer II
TGN	Trans Golgi Network
VSR	Vacuolar Sorting Receptor
YFP	Yellow Fluorescent Protein
YT	Yeast extracts Tryptone

1. INTRODUCTION

1.1 The secretory pathway

Eukaryotic cells have a complex of endomembranes where proteins, sugars and lipids are synthesized, and along which they are transported and modified (Palade, 1975; Staehelin, 1997). This endomembrane system is named secretory pathway and its main organelles are the endoplasmic reticulum (ER), the Golgi apparatus, Trans Golgi Network (TGN) vacuoles and plasma membrane. Intracellular trafficking is mediated by vesicles which shuttle cargo molecules (proteins, polysaccharides and lipids) between these organelles. Notwithstanding the general high homology of the gene involved in the secretory pathway between plant, mammalian and yeast; the intracellular organization of plant cells is different, specifically planned in order to have protein sorting to different vacuoles and the correct orientation for cell division (Brandizzi and Hawes, 2004).

Proteins synthesized at the ER surface directly proceed to the Golgi apparatus (Vitale and Denecke, 1999; Neumann et al., 2003). But some storage proteins can be directly transferred from the ER to the storage vacuole (fig. 1.1, arrow 1), storage proteins can also reach the storage vacuole living from the *cis* and *trans* Golgi apparatus compartments (fig. 1.1, arrow 2). Usually cargo for the exocytotic route, as well as for the lytic vacuole is sorted mainly from the TGN (fig. 1.1, arrow 3 and 4) by a receptor mediate transport through clathrin vesicles. In particular proteins addressed to the lytic vacuole have to cross an intermediate compartment which is the PVC. During endocytosis, the material recycled from the plasma membrane or coming from the outside of the cell is internalized in endosome-like compartment (fig.1.1, arrow 5) and form here, probably to the PVC (fig.1.1, arrow 6). Due to the poor knowledge on vesicles role

involved in endocytotic material transfer between endosome, PVC and lytic vacuole, this part of the secretory pathway still requires further investigation.

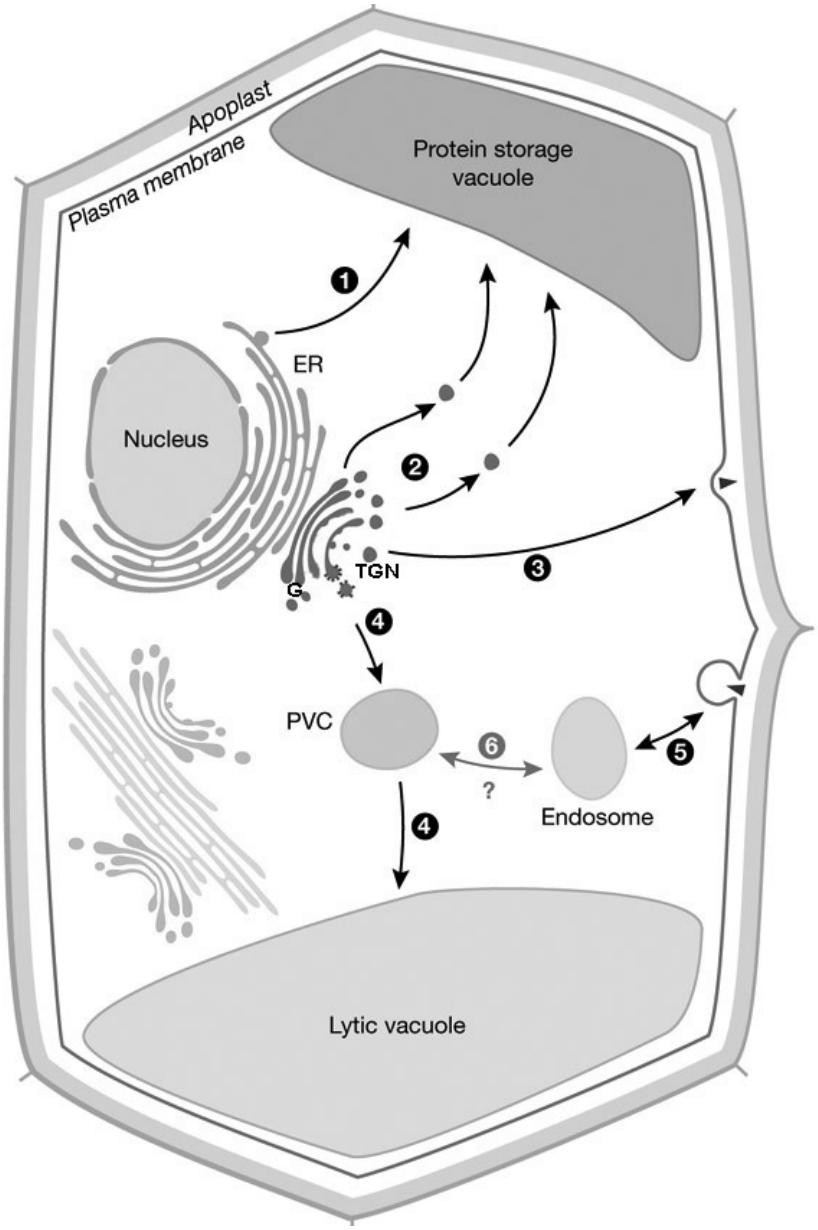

Fig 1.1: Secretory pathway map of higher plants.

ER: endoplasmic reticulum; G: Golgi apparatus; TGN: Trans Golgi Network; PVC: Prevacuolar compartment. The arrows represent the different routes. Route 1 represent traffic from ER to storage vacuole, route 2 from the *cis* and *trans* Golgi apparatus to the storage vacuole; route 3 from the trans Golgi to the plasma membrane; route 4 from the trans Golgi to PVC and lytic vacuole; route 5: endo/ exocytotic route from plasma membrane to endosome and vice versa; route 6: endo/ exocytotic route from endosome to the PVC and vice versa. Figure modified from Brandizzi and Hawes, 2004.

1.1.1 Endoplasmic reticulum

The ER is an organelle that has a large membrane surface that encloses a lumen containing soluble proteins. This membrane system is in continuity with the nuclear envelope (NE), and in plant cells, it extends to adjacent cells through the plasmodesmata (Staehelin, 1997). In the ER membrane are integrated several types of integral and peripheral proteins (Staehelin, 1997; Vitale and Denecke, 1999). Two different types of ER are identified based on the presence or not of ribosomes on distinct areas of its membranes: the smooth endoplasmic reticulum (SER), without associated ribosomes; and the rough endoplasmic reticulum (RER) with associated ribosomes (Palade, 1975).

In plant cells the ER has morphologically different domains with different and specific functions (Staehelin, 1997). ER is responsible for synthesis, processing and sorting of proteins, glycoproteins and lipids (Vitale and Denecke, 1999). Proteins are exported only when they are in the right folded conformation. To exit from the ER they are packaged into vesicles and exported from the ER to the Golgi apparatus (Stephens et al., 2000).

1.1.2 Golgi apparatus

The Golgi apparatus is one of the most studied organelles because it is involved in both secretory and endocytic pathways (Glick and Malhotra, 1998; Neumann et al., 2003). In plant cells, the Golgi apparatus is the main organelle for the production of glycolipids and glycoproteins, destined to the plasma membrane, cell wall and storage vacuoles. It also synthesizes cell wall polysaccharides (Neumann et al., 2003).

The Golgi apparatus is a sort of compact cisternae sequence. This structure is polarized and is made of *cis*, *medial* and *trans* cisternae. The *cis* face communicates and exchanges proteins and lipids with the ER, *medial* Golgi contains particular enzymes for proteins modifications like the removal of mannose and the addition of N-acetilglucosamine (Griffith, 2000), the *trans* face is involved in transport to the TGN (trans Golgi network) (Latijhouwerrs et al., 2005). Proteins that come out from the ER and reach the *cis* face of the Golgi apparatus, passing through the *medial*, undergo post-translational modification. When they are finally at the TGN, secretory cargo is sorted to the final destination inside the cell. Golgi apparatus structure is not the same in all organisms: in mammalian cells it has been described as a group of several stacks composed by flat cisternae interconnected by tubular networks (Rambourg and Clermont, 1990), in yeast cells it exhibits single layers of Golgi apparatus cisternae spread throughout the cytoplasm (Preuss et al., 1992; Rossanese et al., 1999). In plants, the Golgi apparatus is organized as small cisternae stacks sprinkled in the cytoplasm in close association with the ER network. Notwithstanding the differences in structural arrangement of this organelle among the three mentioned species, the dynamics of this organelle are conserved.

The structure of the Golgi apparatus is preserved by a matrix of resident proteins (Slusarewicz et al., 1994; Seemann et al., 2000; Renna et al., 2005). The integrity of the Golgi apparatus structure depends on a perfect equilibrium between the anterograde and retrograde membrane flow (Lippincott-Schwartz et al., 2000; Shorter and Warren, 2002), and interrupting this equilibrium by drugs that interfere in this vesicle traffic, the Golgi apparatus organization is compromised. One of these drugs is brefeldin A (BFA), this

fungal metabolite hampers the activity of ARF1, which regulates the retrograde pathway (Klausner et al., 1992; Satiat-Jeunemaitre and Hawes, 1992; Stefano et al., 2006).

1.2 Post Golgi compartments in the plant secretory pathway

1.2.1 Trans Golgi Network (TGN)

TGN is one of the most studied organelles of the past few years. The TGN is in charge of the major sorting event in the cell. Recent studies on plants show microscopic evidence that the Golgi apparatus and the TGN are distinct entities (Dettmer et al., 2006; Lam et al., 2007b). The electron microscope allowed the identification of an additional cluster of vesicular and tubular structures, morphologically comparable to the TGN, named partially coated reticulum (Staehelin and Moore, 1995; Lam et al., 2007b). Since the partially coated reticulum and TGN are so similar and so close to the *trans* side of the Golgi, it has been suggested that they are two functional domains of the same organelle. Alternatively they can be considered as two developmental stages of the same organelle, assuming that TGN could mature into partially coated reticulum (Lam et al., 2007a).

1.2.2 Prevacuolar compartment (PVC) and vacuole

Following the secretory route, between the TGN and the vacuole, there is the PVC (fig1). Due to their acidic environment, the PVCs are able, after the internalization of the vacuolar sorting receptor (VSR) with their ligand, to separate the receptor and the ligand and to recycle the receptor to the Golgi apparatus (daSilva et al., 2005). Furthermore, it has function in capturing and returning missorted luminal proteins to the Golgi apparatus. Plant cells have two different types of vacuoles: a storage vacuole (SV) and lytic vacuole (LV) (Paris et al., 1996). Proteins addressed to the storage vacuole are exported from the

TGN by vesicles. In some cases, the storage route can bypass the TGN and proteins can be exported directly from the cis side of the Golgi apparatus or from the ER if the proteins do not require Golgi mediated modifications (Hinz et al., 1999; Hillmer et al., 2001; Saint-Jore-Dupas et al., 2004). On the TGN there is a family of vacuolar sorting receptors (VSR), which are involved in clathrin coated vesicles transport to the lytic vacuole (Kirsch et al., 1994; Paris and Neuhaus, 2002). In *A. thaliana,* budding of clathrin-coated vesicles from the TGN is possible in the presence of a protein called dynamin-like 6 (ADL6). This protein is specifically involved in the traffic directed to the lytic vacuole; mutants for this protein block the transport to the lytic vacuole but not the traffic to the plasma membrane (Jin et al., 2001). Therefore, the TGN operates as a sorting compartment from which, depending on the destination organelle, protein transport is mediated by different and specific vesicles.

It is not yet known whether once on the PVC, the release of the cargo to the lytic vacuole requires additional organelle modification like maturation or membrane fusion (Hanton et al., 2007). From studies in germinating seeds of protein storage vacuoles, it has been discovered that both sorting pathways and processing proteins join the storage PVC (Otegui et al., 2006; Wang et al., 2007). It remains unclear how proteins designated for different vacuole types and delivered to the same compartment, might be segregated. Recently new SNAREs mediating the sorting for the lytic and storage vacuole (Sanmartin et al., 2007), have been identified in *A. thaliana*. Furthermore, a specific role has been demonstrated for the SNARE SYP21 in PVC to lytic vacuole transport (Foresti et al., 2006). These findings suggest that different and specific SNAREs can allow specificity

of the protein sorting to the different vacuoles, explaining potential machinery for vacuolar protein sorting from the PVC to the lytic vacuole or to the storage vacuole.

1.2.3 Plasma membrane

The machinery involved in transport and delivery of secretory proteins and polysaccharides between TGN and the plasma membrane, as well as the targeting signals involved in this process are still unknown in plant cells. Cytochemical and immunolocalization studies on tobacco cells demonstrated that this transport is mediated by uncoated secretory vesicles (Staehelin, 1991; Hadlington and Denecke, 2000).
In tobacco protoplast, it has been recently demonstrated that polysaccharides and proteins are transported to the plasma membrane via two different pathways (Leucci et al., 2007). The final localization of type I transmembrane proteins, is influenced by their length (Brandizzi et al., 2002). For transport to the plasma membrane of multispanning proteins the integrity of the cytosolic domain appear to be fundamental (Lefebvre et al., 2004). Proteins involved in the traffic to the plasma membrane are adaptins, SNARE proteins (soluble N-ethyl-maleimide sensitive factor attachment protein receptors) (Uemura et al., 2004), dynamins, RABGTPases, GEF proteins (guanine exchange factors) and other small GTPases like ARF (ADP ribosilation factors). The *A. thaliana* genome encodes for several ARFs but, experimental confirmation for the involvement of specific ARF candidates in the endocytic machinery is limited as is knowledge about how they can be related to transport to the plasma membrane or to other organelles of the post Golgi secretory pathway.

1.2.4 Endosomal compartments

In mammals and yeast, endosomal compartments have been identified and discriminated by suitable markers (Gruenberg, 2001; Raiborg et al., 2003). In contrast, in plant cells the endosomal compartments, due to a lack of appropriate markers, are still poorly defined. In plant systems, four endosomal compartments have however been identified: The early endosome, recycling endosome, late endosome and secretory endosome, but their structure is not well defined.

The early endosomes operate as the first sorting station for the newly internalized cargo; it is thought that they are involved in the traffic of cargo that needs to be quickly re-cycled to the plasma membrane.

The recycling endosomes are implicated in recycling and secretion of cargo to the plasma membrane.

The late endosomes are the equivalent of the PVCs (Tse et al., 2004), and are the place where endocytic and secretory pathway converge (Samaj et al., 2005).

The secretory endosomes take part in the post Golgi secretory event (exocytosis) budding from their membrane secretory vesicles or blending completely with the plasma membrane (Samaj et al., 2005).

1.3 Endocytic pathway

Endocytosis is a process involved in the uptake of molecules from outer surface of the plasma membrane. This process has very important roles in signalling, Ca^{2+} regulated secretion and vesicle cycling. Due to the existence of a very tight link between proteins involved in endocytic/exocytic pathways and human cancer (Floyd and De Camilli, 1998;

Hyun and Ross, 2004), the understanding of this process generates much interest. For a long time it was believed that in higher plants, the endocytosis would not work because of the high turgor pressure. Only recently, plants have been considered a useful model system for cell-cell communication and endosome signalling studies (Geldner, 2004; Samaj et al., 2004; Murphy et al., 2005).

One of the mechanism by which, yeasts, animals and plants can internalize plasma membrane proteins and extracellular cargo by clathrin-coated vesicles. The evidence that the molecular machinery of the clathrin dependent endocytosis is conserved in plants is due to the identification of most of the proteins involved in the clathrin dependent endocytosis in yeast and animal (Holstein, 2002; Barth and Holstein, 2004). Some of these proteins identified in plant cells, are clathrin, AP180 (adaptor protein), two adaptins, dynamins and other proteins containing the SH3 domain (src Homology-3), which is important to bind adaptor proteins.

Furthermore the finding that the diameter of clathrin-coated vesicles in plant cells is smaller (70-90 nm) compared to animal cells (120 nm) justify the endocytosis despite the high turgor pressure in plant cells (Meckel et al., 2004). Since the studies of endocytosis in plants are relatively at the early stages, very few endosome markers have been identified. Some specific molecular markers used for plant endosome are three different RABGTPases: ARA6, ARA7 and RHAI.

In addition to these molecular markers, some membrane selective FM-dyes are used to monitor endocytosis and exocytosis. One of these is the FM4-64 that depending on the exposure time marks the endocytic organelles and the vacuole. The other FM-dye is FM1-43, which is less used because its behaviour is different in different cell types: in

BY2 cells it seems to be a good marker with the same distribution of FM4-64 but in turgid guard cells it sometimes labels the mitochondria (Emans et al., 2002; Ovecka et al., 2005). Notwithstanding the identification of these few markers the post Golgi organelles functions, structures and organization is still very confusing.

1.4 Secretory pathway versus endocytic pathway

1.4.1 Post Golgi protein traffic: small GTPases role

In order to have a well-organized traffic between all the organelles of the secretory pathway, small GTPases members of the Ras superfamily like RAB and ARFGTPases are required. In plants, more isoforms of these GTPases have been found and for most of them, the function has yet to be fully defined (Hanton et al., 2007).

1.4.2 RABGTPases

The Arabidopsis genome contains at least 57 loci encoding for presumed RAB proteins (Rutherford and Moore, 2002; Vernoud et al., 2003). Studies on RAB proteins in plant demonstrate that they regulate specific steps of the secretory pathway. RABD2a and RABB (respectively Rab1 and Rab2 in mammals) are implicated in the ER to Golgi transport (Batoko et al., 2000); RabE1d is involved in the traffic between the TGN and the plasma membrane (Zheng et al., 2005), while RHAI (one RAB5 homologue in mammals) controls soluble cargo traffic between the PVC and the lytic vacuole (Sohn et al., 2003).

RABF1 (ARA6) and RABF2 (ARA7) only partially colocalize each other (Ueda et al., 2004) and with the FM4-64 dye the colocalization is not complete (Ueda et al., 2001).

These discoveries not only confirm the existence of different endosomal compartments within the cell, but also that these different endosomal compartments interact with each other.

ARA7 and RHAI localize both at the early and late endosome, suggesting a maturation of the early endosome to late endosome (Lee et al., 2004; Ueda et al., 2004). RHAI is considered also a PVC marker (Sohn et al., 2003).

ARA6 in part colocalize with the SNAREs proteins SYP21 and SYP22 on the PVC, (Sanderfoot et al., 2001), on the other hand, RABF2b partially colocalizes with SYP21 (on the PVC) and with the vacuolar sorting receptor BP80 (on the PVC and Golgi apparatus). A partial colocalization of ARA6 and RABF2b on the PVC lead to conclude that this compartment as well as the TGN could take part in both the secretory and endocytic pathways.

1.4.3 ARF (ADP Ribosylation Factors) GTPases

The GTPase (small guanosine triphosphates) proteins act as molecular switches and regulate protein-protein interactions controlling the intracellular trafficking. These proteins define the identity of the secretory organelles and control the specificity of the fusion vesicle-membrane (Munro, 2002). These small GTPases are highly conserved among the kingdoms (Munro, 2005). It is already known that their anchoring to the membrane is due to lipid adaptations (Serafini et al., 1991), but their correct targeting is still unknown. The N-terminus of ARF proteins is myristoylated; they are specifically characterized by an amphipatic helix that is formed by the first 12-18 residues.

These proteins, switch from the inactive form (GDP-ARF) to the active form (GTP-ARF) by guanine nucleotide exchange factor (GEFs) and then again to the inactive form (GDP-ARF) by GTPase activating proteins (GAPs) which facilitate the GTP hydrolysis activity of ARF (fig 1.2). Switching between the active and inactive forms, ARFs regulate the assembly and the disassembly of the coatomer proteins (fig 1.3).

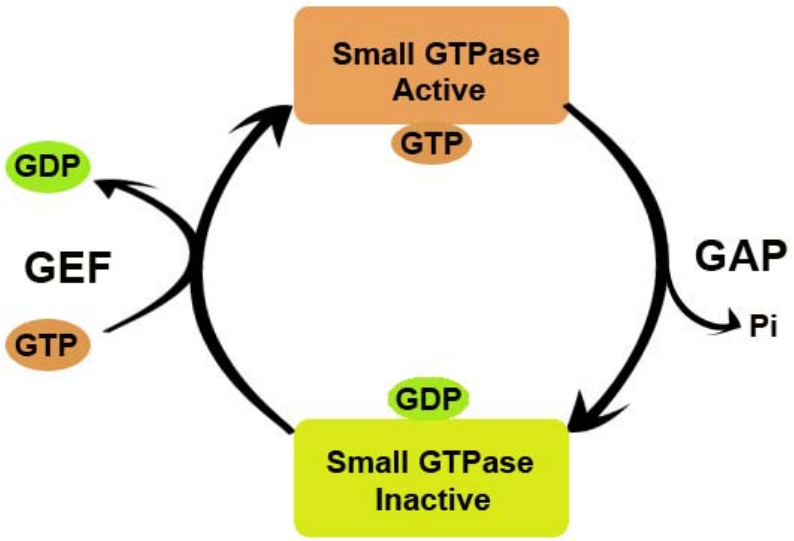

Fig 1.2: Diagram explaining the GDP/GTP molecular switches for GTPase proteins.

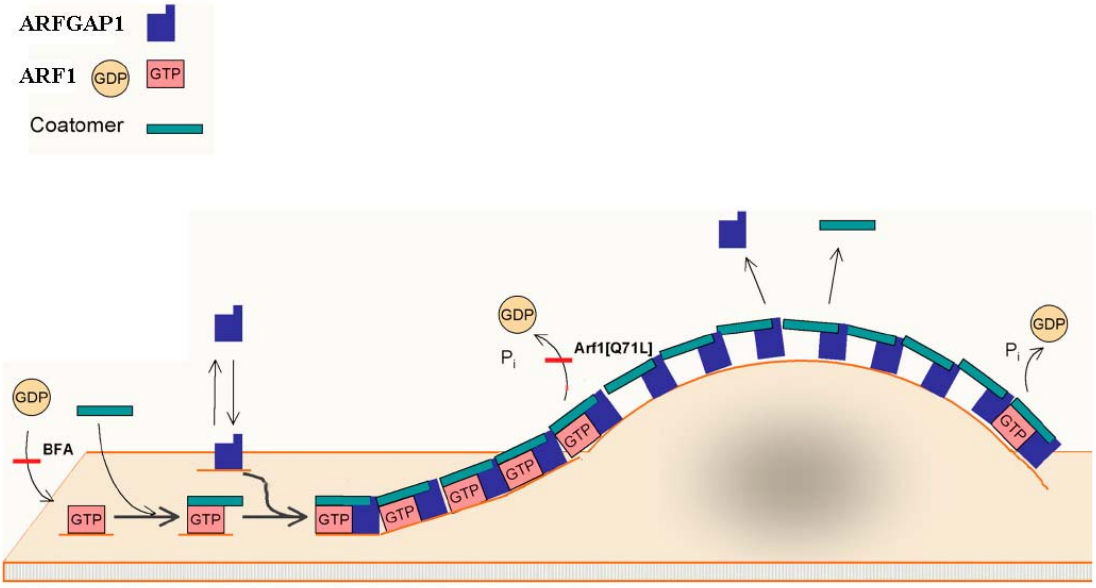

Fig 1.3: Schematic representation of ARF recruiting on the membrane.

Picture adapted from Liu et al 2005.

When the protein is in the GDP form, the hydrophobic side of the helix is covered in a binding pouch, and the protein detaches from the plasma membrane (Beraud-Dufour et al., 1999; Pasqualato et al., 2002). Specific GEFs (guanosine exchange factors), recognize the ARFs and stimulate a conformational modification in the GTP form, which expose the amphipatic helix. In this conformation state, the myristoylation at the N-terminus allows the binding to the membrane (Mossessova et al., 2003; Renault et al., 2003).

The Arabidopsis genome encodes for twelve ARFs, in which more of the important regions are conserved also in mammals and yeasts (Gebbie et al., 2005).

Differently from other GTPases like the RABs that operate at single step in membrane trafficking, Arfs usually act at multiple steps. An example is ARF1 that regulates the creation of coat protein complex I (COPI) coated vesicle (Pimpl et al., 2000), which have function in the retrograde Golgi apparatus to ER traffic, and are also important for the anterograde transport and in the maintaining of Golgi apparatus integrity (Ritzenthaler et al., 2002; Stefano et al., 2006). ARF1 is also fundamental in the formation of adaptor complex/clathrin-coated vesicle (Zhu et al., 1998; Bigay et al., 2003; Nie et al., 2003; Wennerberg et al., 2005), in this way it mediates the budding vesicle at the TGN.

ARFs target different organelles in the same cell, and Arfs homologues target different organelles in different cell systems (Vernoud et al., 2003; Memon, 2004).

An example is ARF1 that in mammalian cells localize at the Golgi membranes, while in plant cells targets the Golgi apparatus and possible post Golgi structures, which may be involved in endocytosis (Xu and Scheres, 2005; Matheson et al., 2007).

It has been recently demonstrated that the amino acid motif MxxE (Methionine-xx-Glutamic acid) is essential for ARF1 to localize to the Golgi apparatus in mammalian cells (Honda et al., 2005). Studies in plant cells have shown that this motif is important not only to localize ARF1 to the Golgi apparatus but also to discriminate the Golgi apparatus from the post Golgi apparatus structures (Matheson et al., 2008). Furthermore, an Arabidopsis plasma membrane ARF has been identified, this protein named ARFB (ARFB1a) is the homologous of the mammalian ARF6. A comparison of the protein

sequence of ARF1 and ARF6 in mammals revealed that the motif MxxE of ARF1 overlaps with a motif IxxD in ARF6 (Honda et al., 2005).

Although plant ARFs involvement in processes like mitosis, cell cycle, intracellular transport, protein-protein interaction and plant defence systems has been observed, the functions of plant ARF proteins are still largely unknown (Lee and Sano, 2007).

1.5 Objectives

The aim of this research is to gather into the molecular mechanisms ARF isoforms in plant cells. This work is focused to investigate a possible involvement of some members of the ARF family in the regulation of endocytic pathway.

A. thaliana genome encodes for 12 ARFs, and for none of them is has been established a well defined role in the endocytic machinery.

.

The objectives of this thesis are:

1. To identify ARF proteins carrying important motif for post-Golgi apparatus addressing
2. To examine their localization in plant cells
3. To study their kinetics
4. To examine their effects on the secretory pathway

2. MATERIALS AND METHODS

2.1 Materials

2.1.1 Biological materials

Nicotiana tabacum plants (cv Petit Havana) were grown in a growth chamber using commercial mix soil. The growth conditions used were: 16 hours in the light at 27 ºC and 8 hours in the dark at 24 ºC, at a light irradiance of 200 μE. m^{-2}. sec^{-1}. The plasmids, *Agrobacterium tumefaciens* and *Escherichia coli* strains used in this work, are listed in Table A1. The multiple cloning sites of different plasmids are shown in Figure A1 and A2. The cDNA for AtArf1 (At2g47170), AtArfB1a (At2g15310), AtArfB1b (At5g17060) and AtArfB1c (At3g03120) were purchased from RIKEN bio-resource centre (http://www.brc.riken.jp/lab/epd/Eng/).

2.1.2 Solutions, enzymes and primers

The solutions used in this work are listed in Table A2.

Pfu DNA Polymerase, Ribonuclease A (RNase A), and restriction enzymes were purchased from Fermentas (www.fermentas.com). T4 DNA ligase was purchased from Invitrogen (www.invitrogen.com).

The primers used for PCR reactions were purchased from Invitrogen and they are listed in Table A3.

2.1.3 Chemicals

The GFX PCR DNA and gel band purification kit, used for DNA purification, was purchased from Amersham Biosciences (www.amershambiosciences.com).
All other chemical reagents were purchased from VWR (www.vwr.com) and Sigma (www.sigma-aldrich.com).

2.1.4 Media

All the media used in this work are listed in Table A5. LB (Luria Bertani) medium was used to grow *E. coli* and *A. tumefaciens.* The antibiotics (kanamycin, ampicillin or gentamycin) were included in the medium to select specific resistances. YT (Yeast extract Triptone) medium was used to prepare chemically competent *E. coli* MC1061.

2.2 Methods

2.2.1 Bioinformatics

Based on the accessible literature references, four known ARF protein sequences, which are classified as small GTPases were collected. The functional protein sequence in FASTA forms for these genes are collected from NCBI (National Centre for Biotechnology Information) (http://www.ncbi.nih.nlm.gov).
Using ClustalW (http://www.ebi.ac.uk/clustalw), these sequences were used for the multiple sequence alignment (it analyzes the best match for the selected sequences, and lines them up so that the identities, similarities and differences can be seen).

Then a phylogenetic tree was derived (http://www.genebee.msu.su). The phylogenetic tree shows the distance between the protein sequences. Additionally, a tool for predicting functional sites in eukaryotic proteins was used (http://elm.eu.org/).

2.2.2 PCR (Polymerase Chain Reaction)

The PCRs set up, were performed as listed in Table A6. All the PCR reactions were run in a MyCycler thermal cycler (www.biorad.com). The reaction conditions used are described below.

The reaction starts with DNA template denaturation at 94 º C for 4 min; the successive step consists of 3 stages which are repeated for 20 cycles: the first stage is a denaturation stage carried at 94 º C for 30 seconds. The second stage, the annealing phase usually between 48-55 º C for 30-45 seconds, depends on the primer sequences. The third stage is the elongation phase generally at 72 º C for 30 seconds/1 minute depending on the polymerase efficiency (1 minute for each 500 bp using *Pfu* Polymerase). Then, the final extending phase represents the last step performed at 72 º C for 5 min, to fill-in the protruding ends of newly synthesized PCR products. The reactions were hold at 4 º C until analyzed by gel electrophoresis (refer to section 2.2.5).

2.2.3 Overlapping PCR

Site-directed mutageneses were produced by overlapping PCR. This method creates amino acid substitutions by joining two DNA fragments, created in separate PCR reactions (Higuchi et al., 1988; Ho et al., 1989). The two fragments were amplified, starting from the original template, by using one non-mutagenic in 5’ or 3’ and one

mutagenic primer in 3' or 5'. The fragments were purified by DNA extraction from agarose gel, as described in section 2.2.5. The two products obtained, having a complementary region, were used as new DNA template and overlapped, in a second PCR reaction, using as primers the two non-mutagenic primers in 5'end and 3'end.

2.2.4 Mutations created in ARF1, ARFB1a, ARFB1b, and ARFB1c proteins

Overlapping PCR was used to create point mutations as described in Table A3 and A4. The insertion of the mutations was confirmed by analysis with an automated DNA sequencer and the data were processed by using Chromas lite software (www.technelysium.com.au)

2.2.5 DNA agarose gel electrophoresis

Agarose gel electrophoresis was used for DNA product analysis and separation. This system allows DNA quantification, and extraction of selected digestion products. Gels were prepared at 1% in TAE buffer and ethidium bromide was added to a final concentration 0.5 µg/ml, which allows DNA visualization by UV light. To prepare samples for electrophoresis, 1/10 of 5 x loading buffer was added. The voltage used for the sample running was 100V for a time variable between 20 and 30 min.

2.2.6 DNA extraction from agarose gel

After the running, the gel was positioned on a transilluminator emitting UV light at 302 nm. The band of interest was excised from the gel using a scalpel blade; and placed on a 1.5 ml eppendorf tube. The DNA fragments were purified from agarose gels using a GFX

PCR DNA and gel band purification kit from Amersham Biosciences. The protocol was provided by the kit.

2.2.7 Vector preparation

The plasmid PVKH18EN6, containing a coding region for a fluorescent protein at the beginning of the polylinker, or at the end of polylinker, were digested respectively with restriction endonucleases, *BamHI-SacI* or *XbaI-SalI* (all the enzymes were purchased from Fermentas). The digestion reaction mix was composed of 0.5 µg DNA, 10x reaction buffers, 40 units restriction enzyme, and distilled water up to a final total volume of 100 µl. The reaction mix was incubated at a temperature of 37 ºC for 1.5 hours.
When the reaction was ended, the DNA was purified by using GFX PCR DNA gel band purification kit. The vectors were loaded on agarose gel and purified as described in section 2.2.6.

2.2.8 Ligation reaction

The ligation reaction requires a clean open vector and a DNA insert previously digested with the appropriate restriction enzymes, and quantified on agarose gels by comparison with the GeneRuler 1 kb DNA ladder. The ligation reaction was assembled thus: 4 µl of 5x ligase buffer, 1 µl of clean open vector (10 ng), 1 unit of T4 DNA ligase and ligated with a five fold molar excess of insert, sterile distilled water up to a total volume of 20 µl. The mixture was incubated at 16 °C overnight in a MyCycler thermal cycler.

2.2.9 Preparation of competent *E. coli* MC1061

E. coli MC1061 cells were streaked on LB plates with streptomycin 50 µg/ml and incubated overnight at 37 °C. A single colony was inoculated in 3 ml YT medium and incubated at 37 °C with shaking at 200 rpm until an $O.D._{.550}$ of 0.300. The culture was then poured into 200 ml of pre-warmed (37 °C) YT medium and incubated at 37 °C with shaking at 200 rpm. When the culture reached an $O.D._{.550}$= 0.480, it was divided into four sterile 50 ml Falcon tubes and left on ice for 5 min. The cells were collected at the bottom of the tubes by centrifugation at 3000 *g* in a Beckman's centrifuge, equipped with a swing out rotor at 4 °C for 20 min, and the supernatant was discarded. Cells were resuspended in a total of 80 ml of ice-cold TFBI buffer and placed on ice for 5 min. The suspension was centrifuged as before and the pellet was resuspended in 8 ml of TFBII buffer and left on ice for 15 min. Aliquots of 100 µl were pipetted into pre-chilled Eppendorf tubes and frozen in liquid N_2. These aliquots were stored at -80 °C.

2.2.10 Competent *E. coli* transformation

To transform *E.coli* MC1061 a heat shock method was used. The frozen aliquots of competent cells (*E. coli* MC1061) were taken from -80 °C and thawed on ice. The DNA, 10 ng plasmid solution or a10 ng ligation mixture, was then added to the competent cells, carefully mixed, and kept on ice for 20 min. The cell suspension was heat-shocked at 42 ° C for 30 seconds and quickly moved on ice for 5 min. LB medium (800 µl) was added to each tube and incubated at 37 ° C for 1 hour with shaking at 170 rpm. The cell suspension was then plated on LB agar plate containing the specific antibiotic for the selection of the inserted plasmid, and grown overnight at 37 °C.

2.2.11 Preparation of competent *Agrobacterium tumefaciens*

A. tumefaciens (GV3101) stored as glycerol stocks at -80 °C, was streaked on LB agar plate containing gentamycin 15 µg/ml. After 48 hours incubation at 28 °C, a single colony was inoculated into 5 ml of LB medium supplemented with gentamycin 15 µg/ml and incubated overnight with shaking at 250 rpm. Two ml of culture were then poured into 50 ml of LB in a sterile 250 ml flask and grown at 28 °C until the culture $O.D._{600}$ was approximately 0.5- 1.0. Then the culture was transferred in ice for 10 min. Cells were collected at the bottom of 50 ml Falcon tube by centrifugation at 4 °C, for 10 min at 5000 rpm. The supernatant was discarded and the cells were gently resuspended in 1 ml of sterile cold 20 mM $CaCl_2$. The cells suspension was then divided in ice-cold eppendorf 1.5 ml tube making 40 µl aliquots that were instantly frozen in liquid nitrogen and stored at –80 °C.

2.2.12 Plasmid DNA extraction (Minipreps)

To isolate the plasmidic DNA from transformed *E.coli* cells, a single colony was selected from the LB agar plate and inoculated into 3 ml of liquid LB, always supplemented with appropriate antibiotic and grown overnight at 37 °C with agitation at 180 rpm. The 3 ml cell suspensions were poured into 1.5 ml sterile eppendorf tubes and centrifuged at 14,000 rpm. After the supernatant removing, the pellet was resuspended in 250 µl of P1 solution supplemented with 50 µg/ml of RNase A (Fermentas) (stock: 10 mg/ml in ddH_2O), and incubated at room temperature for 15 min. Then, P2 (250 µl) solution was added and mixed very carefully, this mix was left at room temperature for 10 min. Finally 350 µl of P3 solution was added, carefully mixed and incubated at 4 °C for 10 min. The

obtained mix was then centrifuged at 14000 rpm for 10 min. The supernatant (750 µl) was transferred into a new eppendorf tube containing 750 µl of isopropanol. The new mixture was vortexed and centrifuged at 14000 rpm for 30 min for DNA to pellet. The pellet was left to dry at 37 ° C for 10 min, then it was resuspended in 50 µl of distilled water and stored at -20 ° C.

2.2.13 Maxiprep for preparation of high quality DNA

For maxiprep DNA preparation endotoxin free all the indication from QIAGEN plasmid maxi kit (http://www.qiagen.com) protocol book were carefully followed as indicated for high copy plasmid DNA preparation.

2.2.14 Competent *Agrobacterium tumefaciens* transformation

An aliquot of competent *A. tumefaciens* cells GV3101 was taken from the ultra freezer and left on ice to thaw. Then 7 µl of plasmid DNA were added to the competent cells, mixed, and left on ice for 10 min. After that, each tube transformation was quickly immersed in liquid nitrogen for 5 min, directly from liquid nitrogen the cell were taken and transferred and heat shocked at 37 °C for 5 min. Then, LB medium (800 µl) was added to the cells. Cells were incubated for 4 hours at 28 °C with shaking at 120-130 rpm, poured onto selective LB plates, and incubated at 28 °C for two days to obtain visible colonies.

2.2.15 Transient *N. tabacum* plant transformation

Cultures of *A. tumefaciens* were grown at 28 ºC in LB supplemented with kanamycin (100 μg/ml) and gentamycin (25 μg/ml) with shaking at 200 rpm for about 20 hours. Bacterial cells isolated by centrifugation at 8000 g for 5 min at room temperature and resuspended in IF (infiltration buffer) buffer to a final optical density ($O.D._{600}$) of 0.05 for ARFs (wild type and mutants), and SYP61, and 0.2 for ERD2 constructs. The transformed *Agrobacterium* suspension so prepared was injected through the entire leaf into the abaxial air spaces of tobacco leaves by using a sterile 1 ml hypodermic syringe (Kapila et al., 1997). The transformed plant was left in the growth chamber for 48 hours, after that it was ready to be observed to the confocal.

2.2.16 Protoplasts preparation

Sterile *tabacum* leaves were excised from the plant.

The leaves were deprived of the midrib, their abaxial surfaces were riddle using a device consisting of 30 stainless steel needles set into a circular block, and the two halves of the leaf were placed with the abaxial surface downward into a Petri dish containing 7 ml of leaf digestion mix and incubated in the dark overnight. After 12-16 hours incubation, the plates were gently shaken to liberate the protoplasts from the cuticle for 30 min. The resulting mixture was then filtered through a 100 μm mesh filter and rinsed with washing buffer. The protoplast solution obtained was centrifuged in 50 ml falcon tubes in a swing-out rotor (Beckman Allegra centrifuge) at 100 g for 15 min. At this stage the band of floating living protoplast was separated by the rest of the medium with the dead protoplast using a Pasteur pipette connected to a peristaltic pump. The living protoplasts

were resuspended in 25 ml of washing buffer and centrifuged at 100 g for 10 min. The dead cells and underlying medium were removed as before and the entire procedure was repeated twice more. Finally, the protoplasts were resuspended in an appropriate final volume with 300 µl of MMM solution for each transformation.

2.2.17 Protoplasts transient transformation

Protoplast suspension (300 µl) was gently poured into a sterile 15 ml falcon tube using a cut off end tip. A maximum of 20 µg/µl aliquot of plasmid DNA was used for the protoplasts transformation. Polyethylene glycol solution (PEG4000, Fluka) (300µl) was added for direct gene transfer (Di Sansebastiano et al., 1998), and left to incubate for 1 min. Protoplasts were then resuspended in 2 ml of TEX buffer. Two hours later the PEG solution was removed by a rinse with 8 ml of washing buffer by centrifugation. Protoplast were then resuspended in 2 ml of TEX buffer and left at 26 °C in the dark, for 24 hours (all the media compositions are listed in Appendix, table A2).

2.2.18 Harvesting of protoplasts and culture medium

After 24 hours of incubation, the transformed protoplasts suspension was centrifuged in a swing-out rotor at 100 g for 5 min. The floating cell layer was penetrated using a thinned Pasteur pipette and 1 ml of the culture medium was collected into an Eppendorf tube and kept on ice. The remaining cell suspension was diluted 10-fold with 250 mM NaCl, and centrifuged as before. With this procedure all the living and transformed protoplasts move to the bottom of the 15 ml Falcon tube. The supernatant was aspirated with a Pasteur pipette connected to a peristaltic pump without disturbing the pellet, which was

then placed on ice. The pellet was resuspended 500 µl of 0.1 M Na-acetate pH 5 and sonicated for 5 seconds to break the cells. The eppendorfs, the one containing the medium and the one containing the cells were centrifuged at 14000 rpm for 10 minutes at 4 ° C. The supernatant coming from this centrifugation step was poured in new eppendorf tubes and used to measure SecRGUS (Leucci et al., 2007) and α-mannosidase (the constitutive enzyme used as internal control) enzymatic activity. The reaction substrates were 4-methyl-umbelliferyl-β-D-glucuronide (Sigma, Steinheim, Germany) and 4-methyl-umbelliferyla-D-mannoside (Sigma) to measure SecRGUS and α-mannosidase activity, respectively. The reaction were performed at 37°C and stopped at defined slot. The samples were excited at 370nm and the fluorescence emitted measured at 480 nm using a multi-well microplate reader (TECAN Infinite 200) (http://www.tecan.com).

Secretion index (SI) (Denecke et al., 1990) for SecRGUS was estimate as the rate of extracellular activity over the intracellular activity, considering the dilution rate of the incubation medium. As control to quantify the contamination coming from broken cells, it was evaluated the secretion of the marker mannosidase.

2.2.19 Confocal microscopy

The confocal microscopy is a technique based on the ability of fluorescent protein, due to their particular molecular structure, to absorb specific wavelengths light and to emit light at longer wavelength. One of the proteins having these characteristic is the green fluorescent protein, it adsorbs blue light and emits green fluorescence (Morise et al., 1974). A schematic representation of Leica SP5 confocal microscope components is in

Figure 2.2.1. Differently from other confocal system, SP5 Leica is the only one, which has not dichroic filters. The light excitation emitted from the laser passes through a crystal called acoustic optical beam splitter (AOBS). The light reflected by this filter is directed in focus on the pinhole by the objective lens and reach the sample. This means that the focal plane on the sample and the pinhole are confocal, i.e. they are situated on planes conjugated. Therefore, the only light that can cross the pinhole and be collected from photomultiplier comes from the confocal plane.

Transformed leaves were analyzed 48 hours after the *Agrobacterium* mediated transformation. Confocal imaging was performed by using an upright Leica SP5, and a 63 x oil immersion objective. The imaging settings used for GFP and YFP detection were: excitation lines of an argon ion laser of 458 nm for GFP and 514 nm for YFP, used alternately with line switching on the sequential scan facility of the microscope. GFP fluorescence was detected by using a spectral range from 500 to 520 nm, while YFP fluorescence was detected with a 560 to 600 nm spectral range. Using this setting and the sequential scan, communication and bleeding of fluorescence was completely avoided (Hutter, 2004). The cyan fluorescent protein was excited by using a 405 nm violet diode laser and detected by using a 460-530 nm spectral range. In all the figures present in this work, image acquisition was carried out with same imaging settings of the microscope (laser intensity, pinhole aperture, detector gains, zoom and line averaging). To compare the fluorescent proteins expression levels among cells, only cells with similar levels of saturation of the imaging pixels, as determined by the palette function of the microscope software, were acquired (daSilva et al., 2004). Further image handling was performed using Adobe Photoshop imaging suite.

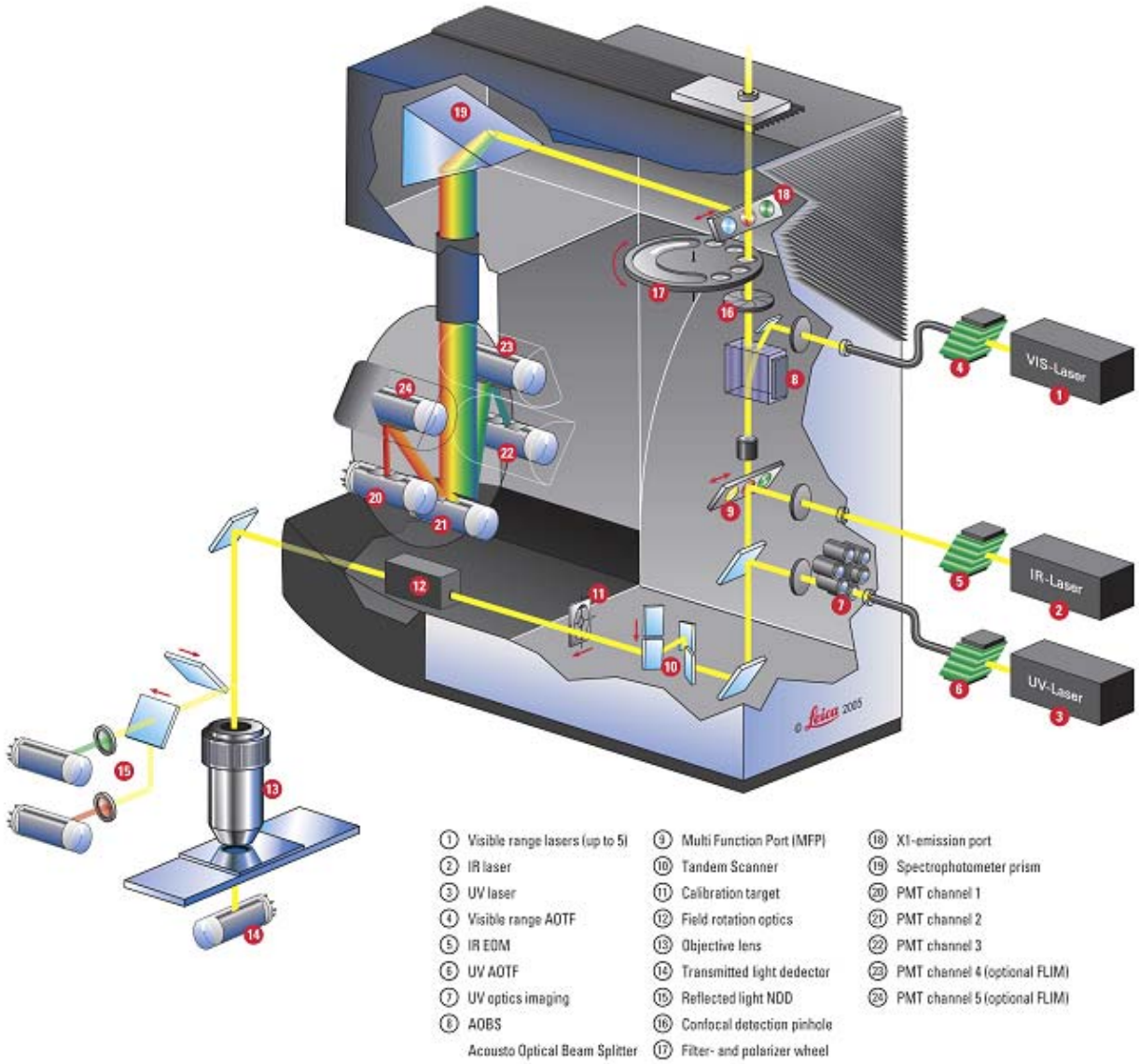

From leica (www.leica.com)

Figure 2.1: Schematic representation of a confocal microscope.

2.2.20 FRAP analyses of GFP fused proteins expressed in leaf epidermal tobacco cells.

The dynamic behaviour of various ARF proteins tagged with fluorescent protein transiently expressed in leaf tobacco cells was examined by FRAP (fluorescence recovery after photobleaching). For live-cell imaging, 3 days old tobacco leaf cells were used. The analyses were performed using a Leica SP5 confocal laser scanning microscope equipped with an argon-krypton laser with a HCX PL APO 63x 1.2-W CORR lens. Prebleach scans were performed at 2% laser power attenuation, 512x256-pixel image size. For bleaching, a pulse at 100% laser power attenuation was used without imaging. The bleach-area has a diameter of 3 μm. The fluorescence recovery period was monitored by collecting images at different times after bleaching. FRAP recovery data were best fitted to a single exponential using IGOR PRO software and the FRAP plug-in written by K. Miura. The ideal plot of a FRAP recovery curve is represented ad described in figure 2.2.

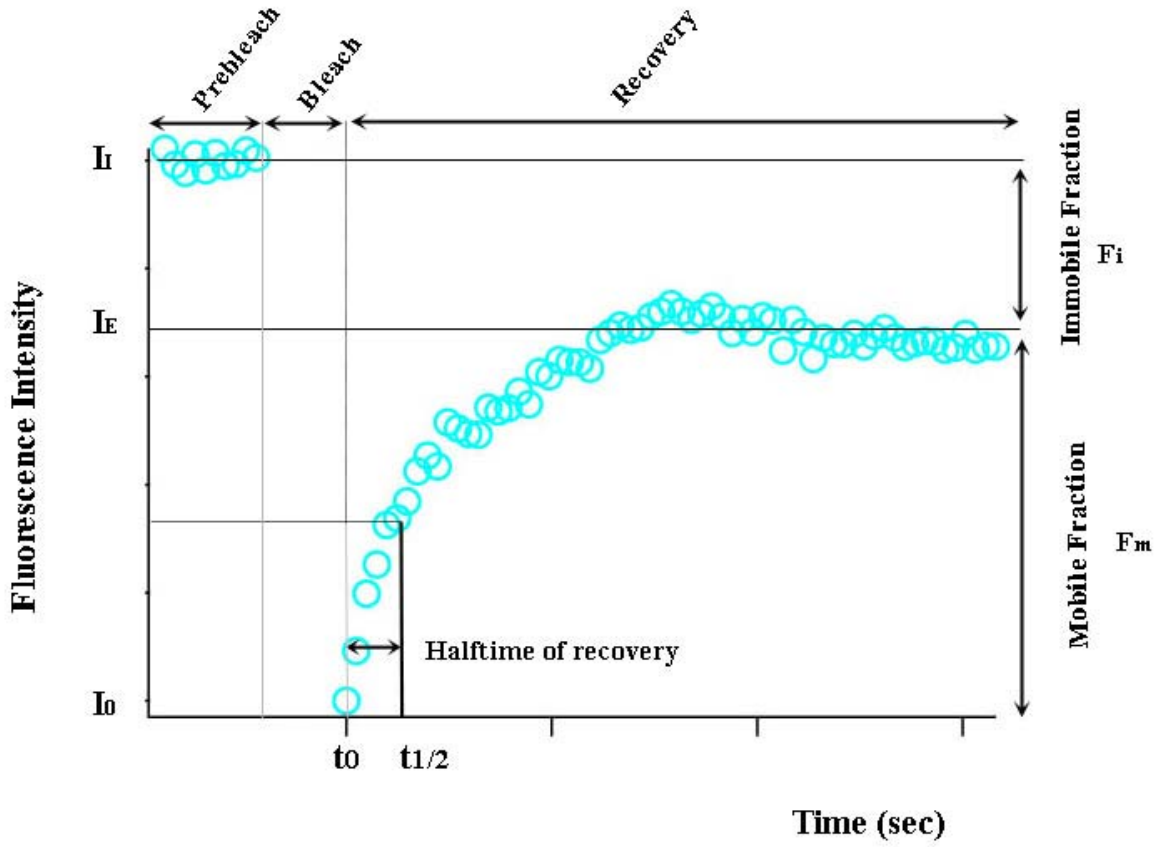

Fig 2.2: Ideal plot of a FRAP recovery curve.

$\mathbf{I_I}$: initial intensity

$\mathbf{I_0}$: intensity at timepoint t0 (first postbleach intensity)

$\mathbf{I_{1/2}}$: half recovered intensity corresponding to t1/2 (I1/2 = (IE - I0) / 2)

$\mathbf{I_E}$: endvalue of the recovered intensity

$\mathbf{t_{half}}$: Halftime of recovery (t1/2 - t0)

Mobile fraction **Fm** = (IE - I0) / (II - I0)

Immobile fraction **Fi** = 1 – Fm

2.2.21 Brefeldin A (BFA) treatment

A little piece of sample, about 2 cm x 2 cm, was cut out from the transformed leaf. This sample was inserted in an eppendorf tube containing a solution of tap water and brefeldin A to a final concentration of 100 µg/ml.

The sample was kept in this solution for 1 hour, protected from the light. When the incubation time was over the sample was poured on a microscope slide and observed.

3. RESULTS

3.1 Bioinformatics analysis of ARF proteins

To identify ARF proteins linked to the endocytic pathway, a ClustalW alignment (http://www.ebi.ac.uk/clustalw) was done. In particular, the motif MxxE of ARF1, important for Golgi apparatus localization and post Golgi apparatus structure discrimination (Matheson et al., 2008) was kept in consideration during the alignment. The BlastP for ARF1 and ARFB1a revealed that the motif ILTD in ARFB1a, which causes the different localization of this protein on the plasma membrane, corresponds to the position of the MxxE motif of ARF1. Using the BlastP analysis other two ARFs have been identified: ARFB1b and ARFB1c, which in the same region have a motif which is different from MxxE but similar to ILTD. The motifs of these proteins are respectively: IIKD and IIRD (figure 3.1). This result is also confirmed and shown in a phylogenetic tree, which describes the two proteins selected for this inquiry as in the nearest branches to the ARFB1a (ARF6 in human) (figure 3.2). Additionally both the proteins possess an additional motif DPF (Brett et al., 2002b), which in human, is important for AP2 interaction. These characteristics suggest that these proteins are good candidates for having a role in the endocytic pathway. Furthermore, among many ARF homologues, phylogenetic analysis revealed that the two selected proteins are most closely related to the ARFB1a for which a role in the endocytic pathway has been already demonstrated (Matheson et al., 2008).

Figure 3.1: ClustalW alignment.

ClustalW alignment of *A.thaliana* ARF1 (At2g47140) with ARFB1a (At2g15310), ARFB1b (At5g17060), ARFB1c (At3g03120), the sequence share high homology and the square underlines the MxxE motif of ARF1, which overlaps with the conserved IxxD motifs in ARFB1a, ARFB1b, ARFB1c

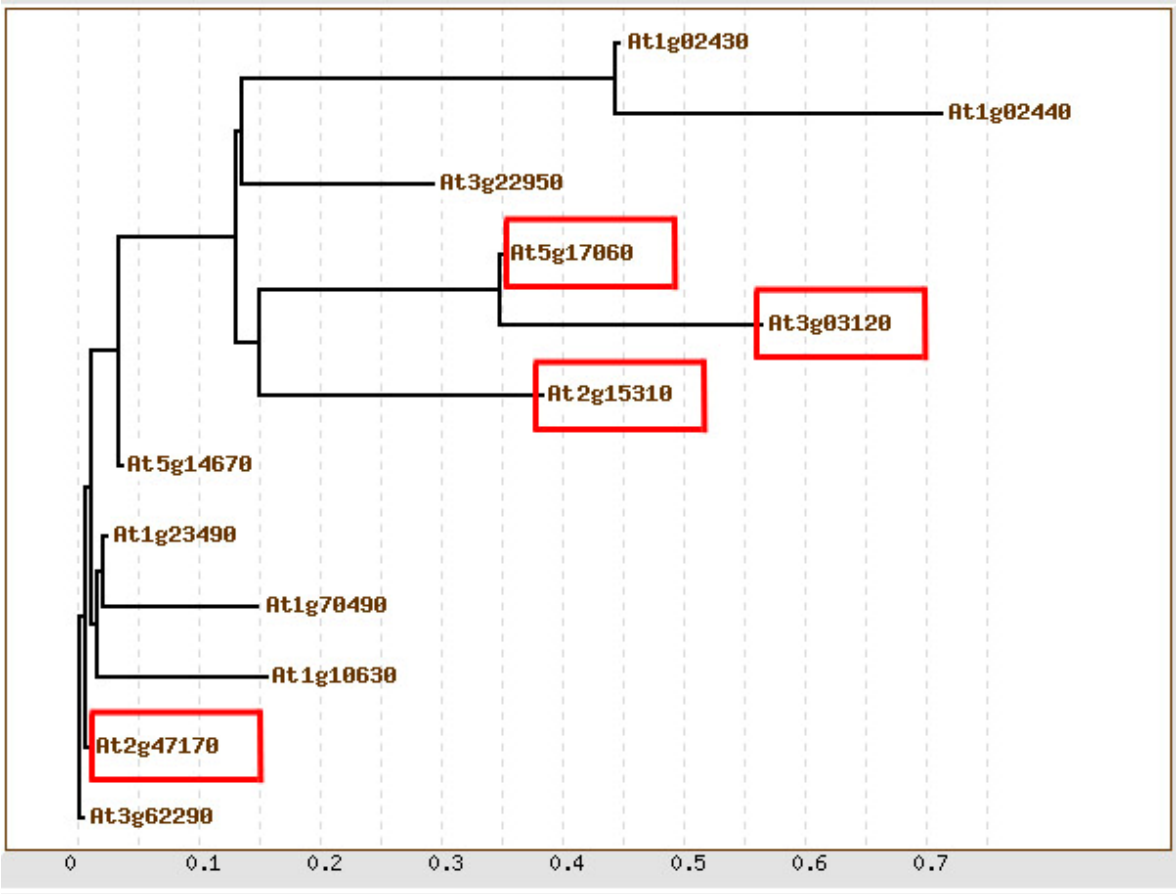

Fig 3.2: Phylogenetic tree.

A neighbour-joining tree of *A. thaliana* ARFGTPases was generated using ClustalW and scoring for amino acid differences (Thompson et al., 1994). The locus highlighted with red squaring are the ones selected as good candidates for endocytic pathway. In particular At5g17060 and At3g03120 are the ones with the branches nearest to At2g15310 (the corresponding of the human ARF6) named ARFB1a in *A.thaliana*, for which a role in the post Golgi apparatus pathway has been demonstrated.

3.2 Subcellular distribution of ARF1, ARFB1a, ARFB1b, ARFB1c in plant cells

One of the aims of this study is to define the cellular role and localization in plant cells of ARFB1b and ARFB1c. The fluorescent protein GFP/YFP was fused to the C-terminus of ARF proteins to preserve the N-terminus, where the amphipatic helix, which is the anchor necessary for the protein binding to the membrane is located. The ARFs fused to the GFP/YFP were expressed transiently in *N.tabacum* leaf epidermal cells.

Laser confocal microscopy analysis indicated that ARF1YFP localizes at Golgi apparatus level (fig 3.3 panels A, B and C) (Stefano et al., 2006) and post Golgi apparatus structure as recently showed (Matheson et al., 2008). Since the punctuate post Golgi apparatus structure of ARF1YFP resemble structures similar to the TGN and/or endosomal compartments, tobacco leaf epidermal cells were cotransformed with different post Golgi structure markers. Using as TGN marker SYP61GFP (fig 3.3 panels E, F and G) (Uemura et al., 2004) in coexpression experiments. Coexpression of ARF1YFP with the Rab GTPase RHAIGFP shows a weak and partial colocalization with this construct (fig 3.2.1 panels Q, R and S). Coexpression experiments of ARF1YFP with FVYEGFP construct (fig 3.3 panels I, J and K) and with ARA7GFP (fig 3.3 panels M, N and O) did not label any overlapping structure.

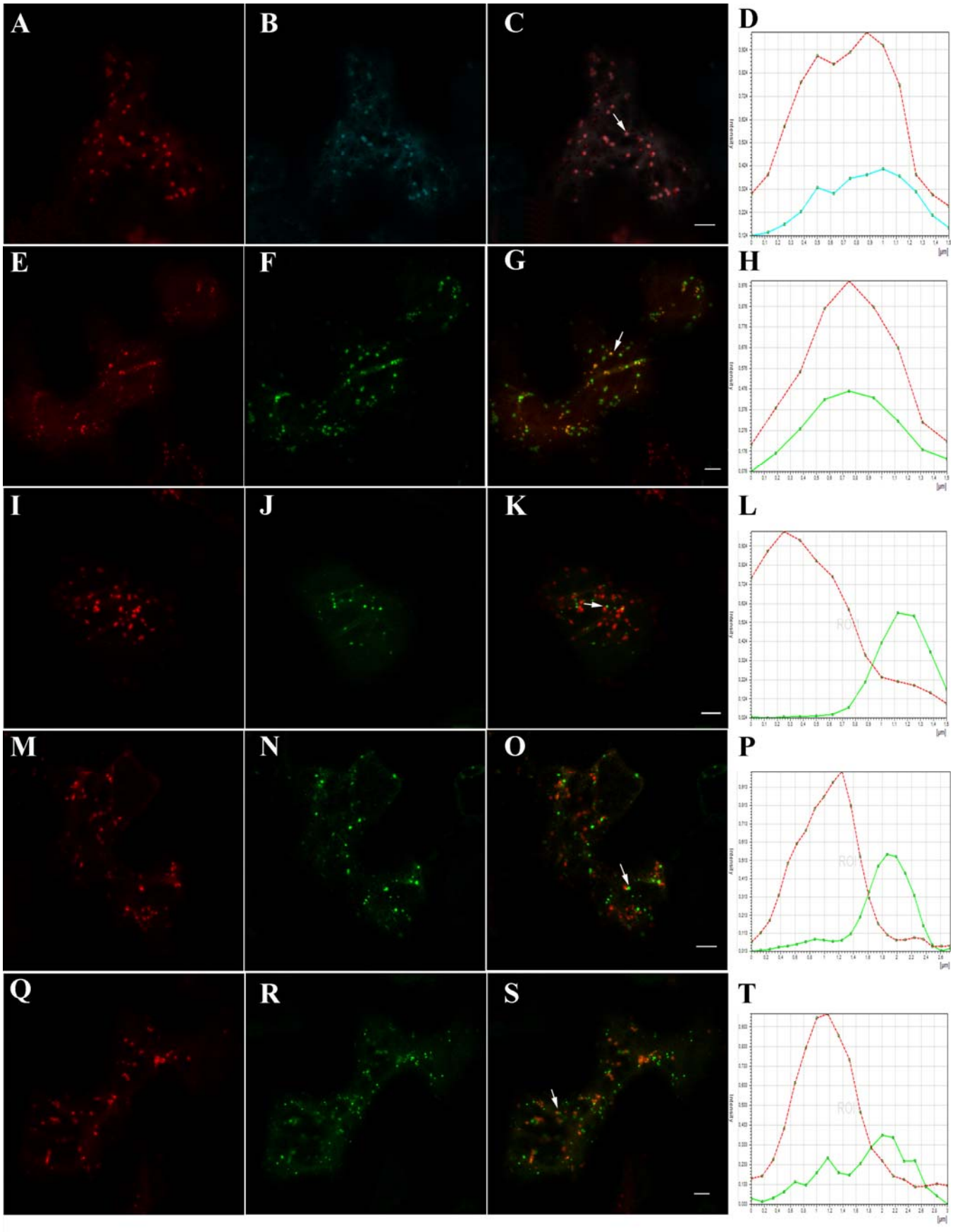
A
B
C
D
E
F
G
H
I
J
K
L
M
N
O
P
Q
R
S
T

Fig 3.3: Subcellular distribution of ARF1YFP.

Confocal images of tobacco leaf epidermal cells, 2 days after *A. tumefaciens* infiltration. ARF1-YFP (A, E, I, M, Q) coexpressed with ERD2CFP (B), SYP61GFP (F), FYVEGFP (J), ARA7GFP (N), RHAIGFP (R). Panels C, G, K, O, S, are the respective merged images, showing the colocalization at Golgi apparatus level (C, D), and TGN level (G, H). The overlap of fluorescence is measured graphically for each experiment at the overlapping structure (arrows) by the distance of the two peaks (panels D, H, L, P, and T). Scale bars = 5 μm.

Next step was to determine in detail the subcellular distribution of ARFB1aYFP which has been shown to localizes at the plasma membrane (Matheson et al., 2008) and labels few punctuate structures. To identify these punctuate structures, ARFB1aYFP was coexpressed with the Golgi apparatus marker ERD2CFP (Boevink et al., 1998), and with SYP61GFP. These experiments demonstrated a colocalization of ARFB1aYFP not with the Golgi apparatus (figure 3.4, panels A, B, C) but with SYP61 (figure 3.4, panels E, F, G), therefore, ARFB1aYFP localizes at the TGN. ARFB1aYFP was also coexpressed with FYVE construct which is a marker for both early, and late endosomes (figure 3.4, panels I, J, K), and with the two RAB GTPases RHAI and ARA7 which are respectively markers for PVC and early/late endosome (figure 3.4, panels Q, R, S and panels M, N, O). For none of these markers a colocalization with ARFB1aYFP was found, this means that this protein does not localize on endosomal or vacuolar compartment.

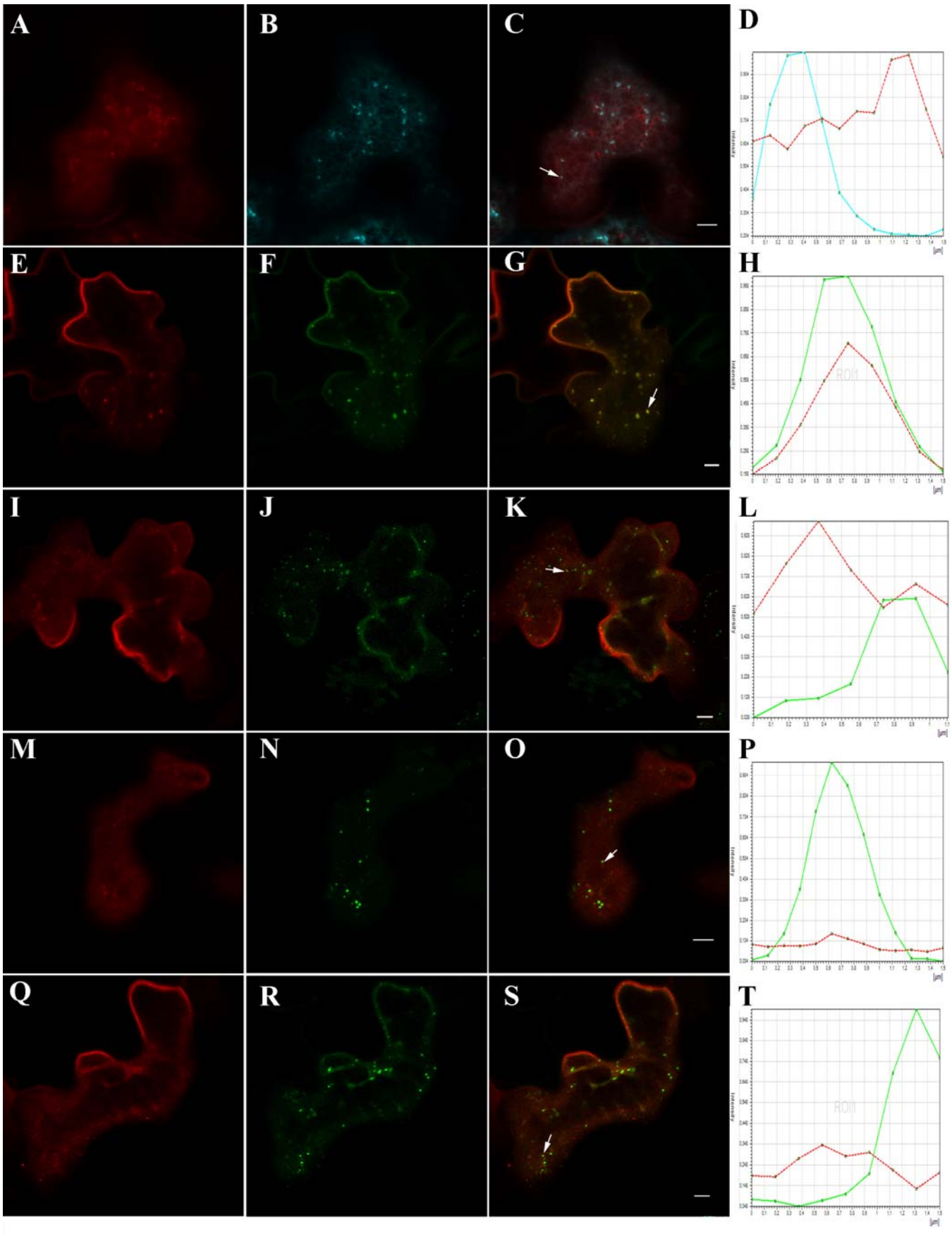
A
B
C
D
E
F
G
H
I
J
K
L
M
N
O
P
Q
R
S
T

Fig 3.4: Subcellular distribution of ARFB1aYFP.

Confocal images of tobacco leaf epidermal cells, 2 days after *A. tumefaciens* infiltration. ARFB1aYFP (A, E, I, M, Q) coexpressed with ERD2CFP (B), SYP61GFP (F), FYVEGFP (J), ARA7GFP (N), RHAIGFP (R). Panels C, G, K, O, S, are the respective merged images, showing the colocalization at TGN level (G, H). The overlap of fluorescence is measured graphically for each experiment at the overlapping structure (arrows) by the distance of the two peaks (panels D, H, L, P, and T). Scale bars = 5 μm.

In the attempt to identify ARF proteins playing a pivotal role into the endocytic pathway, ARFB1b identified by bioinformatics analysis and carrying on the IxxD motif similarly to ARFB1a was investigated by confocal analysis. ARFB1bYFP expressed in plant, localizes diffusely in the cytosol and defines numerous punctuate structures. As these distributions might resemble Golgi apparatus or endosome structures, ARFB1bYFP was coexpressed with the markers for the Golgi apparatus ERD2 (figure 3.5, panels A, B, C) and with the markers for the endosome FYVE (figure 3.5, panels I, J, K) and ARA7 (figure 3.5, panels M, N, O). As for other proteins analysis, ARFB1bYFP was also coexpressed with the PVC marker RHAI (figure 3.5, panels Q, R, S) and the TGN marker SYP61 (figure 3.5, panels E, F, G). ARFB1bYFP shows colocalization only with SYP61, so the punctuate structures that this construct defines, belong to TGN.

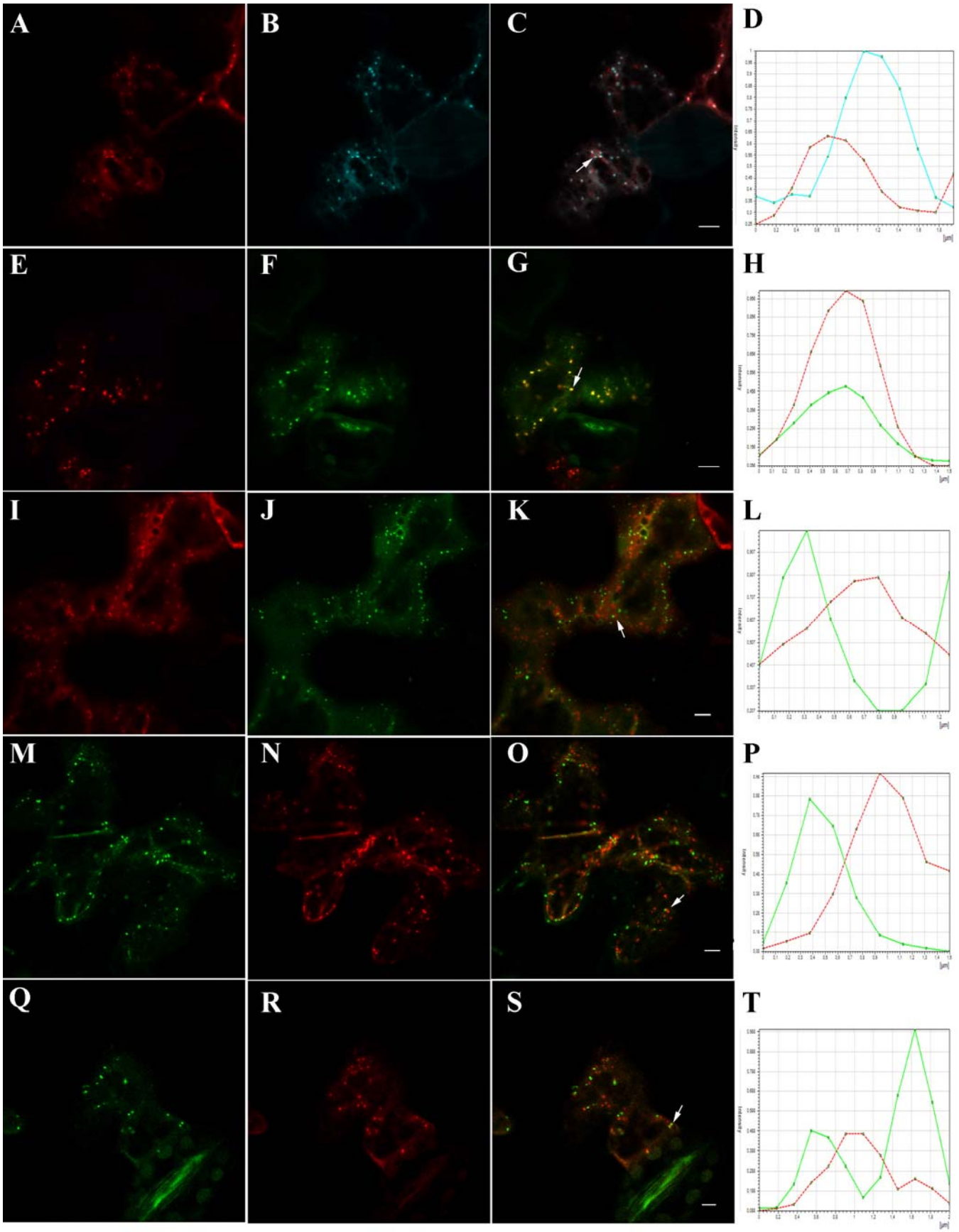
A
B
C
D
E
F
G
H
I
J
K
L
M
N
O
P
Q
R
S
T

Fig 3.5: Subcellular distribution of ARFB1bYFP.

Confocal images of tobacco leaf epidermal cells, 2 days after *A. tumefaciens* infiltration. ARFB1bYFP (A, E, I, M, Q) coexpressed with ERD2CFP (B), SYP61GFP (F), FYVEGFP (J), ARA7GFP (N), RHAIGFP (R). Panels C, G, K, O, S, are the respective merged images, showing the colocalization at TGN level (G, H). The overlap of fluorescence is measured graphically for each experiment at the overlapping structure (arrows) by the distance of the two peaks (panels D, H, L, P, and T). Scale bars = 5 μm

The other protein selected on the basis of its motif similar to the ARFB1a protein, is ARFB1c. For ARFB1cYFP the same experiments were repeated and a slightly different result was found. ARFB1cYFP does not colocalize with the Golgi marker ERD2CFP (figure 3.6, panels A, B, C), colocalizes perfectly with the TGN marker SYP61GFP (figure 3.6, panels E, F, G), does not colocalize with the PVC marker RHAI (figure 3.6, panels Q, R, S), but partially colocalizes with FYVE construct (figure 3.6, panels I, J, K) and ARA7 (figure 3.6, panels M, N, O), leading to the conclusion that ARFB1c localizes at the TGN and also at early, or late endosome level.

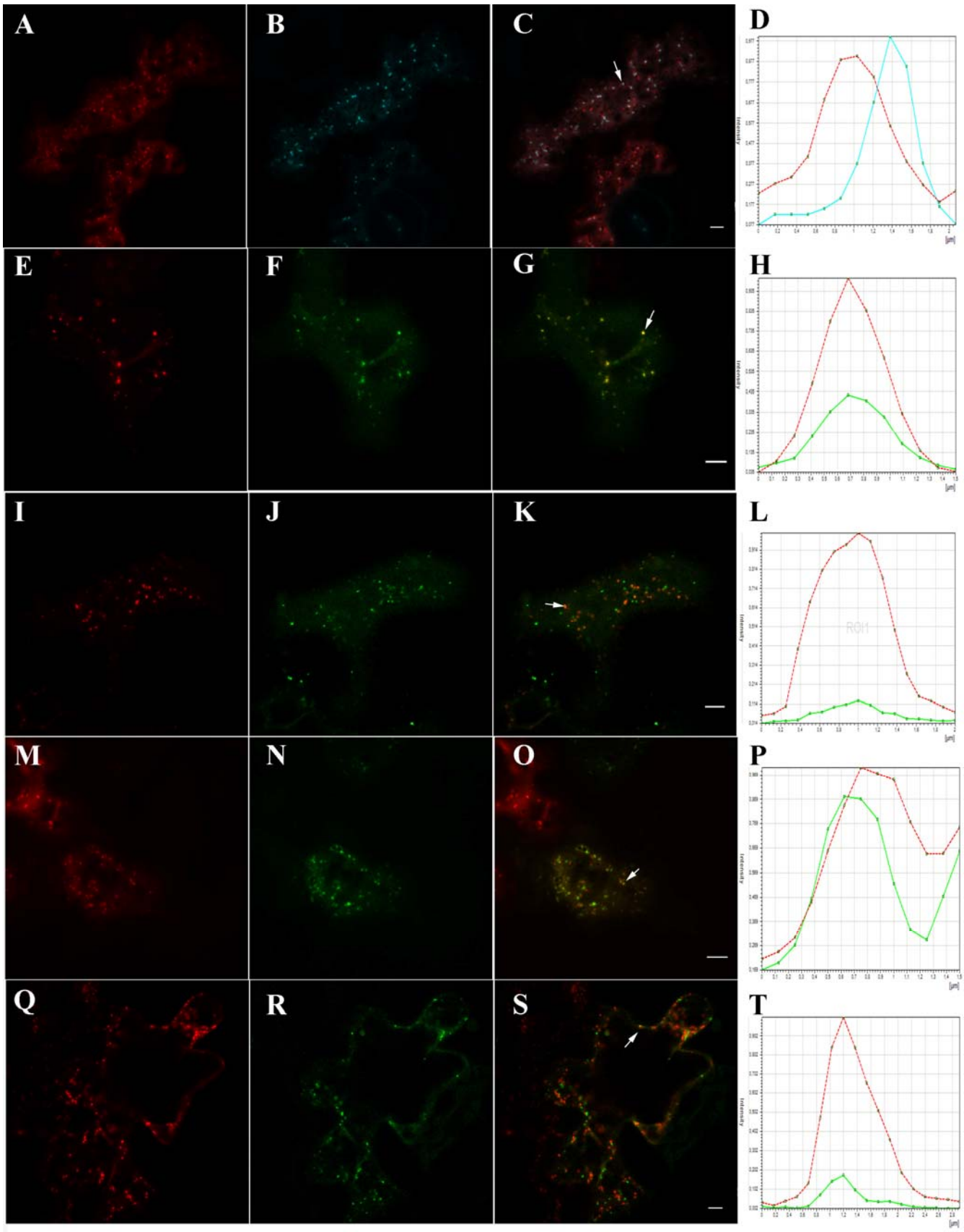
A
B
C
D
E
F
G
H
I
J
K
L
M
N
O
P
Q
R
S
T

Fig 3.6: Subcellular distribution of ARFB1cYFP.

Confocal images of tobacco leaf epidermal cells, 2 days after *A. tumefaciens* infiltration. ARFB1cYFP (A, E, I, M, Q) coexpressed with ERD2CFP (B), SYP61GFP (F), FYVEGFP (J), ARA7GFP (N), RHAIGFP (R). Panels C, G, K, O, S, are the respective merged images, showing the colocalization at TGN level (G, H) and a partial colocalization at early/late endosomes (O, P, S, and T). The overlap of fluorescence is measured graphically for each experiment at the overlapping structure (arrows) by the distance of the two peaks (panels D, H, L, P, and T). Scale bars = 5 μm

3.3 ARF1, ARFB1a, ARFB1b, ARFB1c cross localization

The transient transformation before showed a different localization for the different ARFs. The question now is whether the coexpression of two different ARFs in a transient transformation, it could change drastically the distribution of one of the two proteins, due to a synergistic effect.

To compare more closely the localization of the cloned ARFs, their cross coexpression was done. For this kind of investigation, two ARF proteins at a time were coexpressed, covering all the possible combinations.

This experiment was done also to understand whether the overexpression of one ARF could affect the localization of the others.

The results obtained do not show any change in their localization or in the morphology of the various organelles labelled in the cell with these ARF proteins. These data lead to the conclusion that the overexpression of one ARF protein does not have any effect on the localization of the others. The constructs partially overlap at TGN level (fig. 3.7 and 3.8).

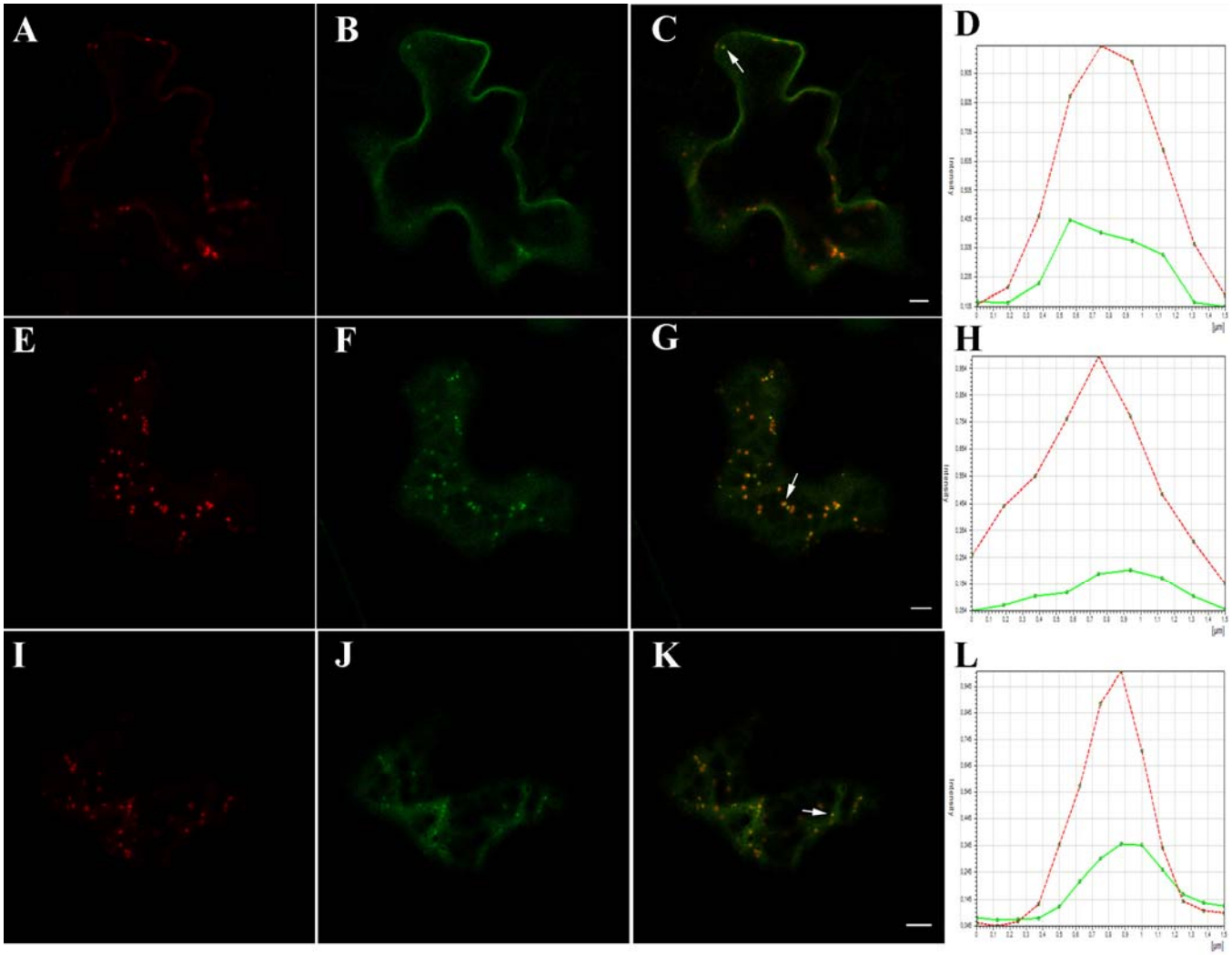

Fig 3.7: Cross coexpression of ARF1, ARFB1a, ARFB1b, ARFB1c.

Confocal images of tobacco leaf epidermal cells, 2 days after *A. tumefaciens* infiltration. ARF1YFP (A, E, I) coexpressed with ARFB1aGFP (B), ARFB1bGFP (F), ARFB1cGFP (J). Panels C, G, K, are the respective merged images, showing the colocalization at TGN level (C, D, G, H, K, and L). The overlap of fluorescence is measured graphically for each experiment at the overlapping structure (arrows) by the two peaks (panels D, H, and L). Scale bars = 5 μm

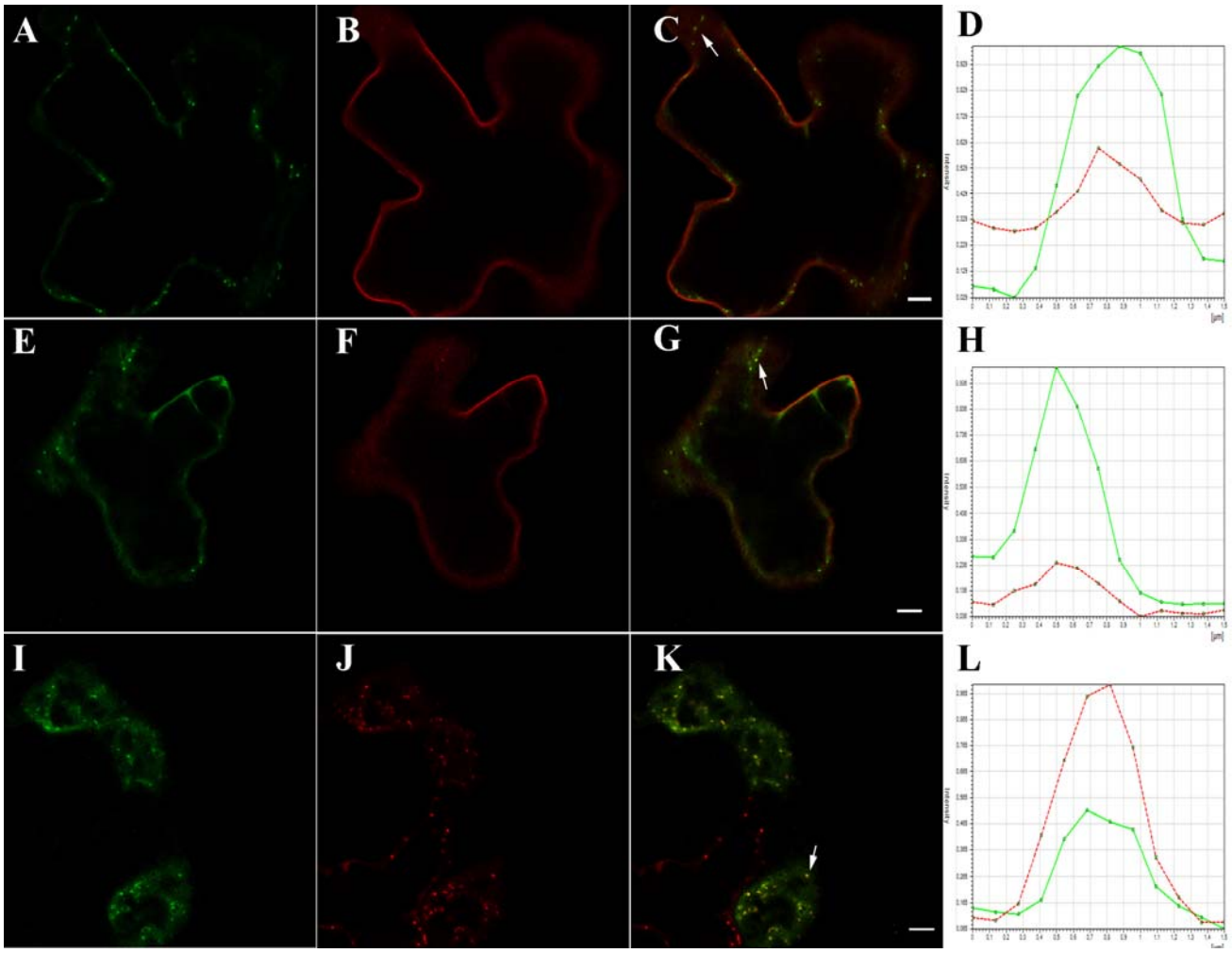

Fig 3.8: Cross coexpression of ARF1, ARFB1a, ARFB1b, ARFB1c.

Confocal images of tobacco leaf epidermal cells, 2 days after *A. tumefaciens* infiltration. ARFB1aYFP (B, F) coexpressed with ARFB1bGFP (A) and ARFB1cGFP (E). ARFB1cGFP (I) coexpressed with ARFB1bYFP (J). Panels C, G, K, are the respective merged images, showing the colocalization at TGN level (C, D, G, H, K, L) The overlap of fluorescence is measured graphically for each experiment at the overlapping structure (arrows) by the two peaks (panels D, H, and L). Scale bars = 5 µm

3.4 Subcellular localization of the ARF1, ARFB1a, ARFB1b, ARFB1c in active and inactive form

To investigate if the active form of ARF1, ARFB1a, ARFB1b and ARFB1c was required to bind to the specific organelles where they localize, some amino acid replacements were introduced. Using PCR mutagenesis, the ARFs were mutated at conserved residues, known either to abrogate GTP binding or to enhance the affinity for GTP.

ClustalW alignments of ARFB1a, ARFB1b and ARFB1c with ARF1, showed the exact position of the residues responsible for GDP and GTP binding. ARFB1a, ARFB1b and ARFB1c blocked in the GDP-bound form were produced by PCR mutagenesis as described in section 2.2.3. The resulting PCR product had a substitution of threonine in position 31 with asparagine (T31N) for Arf1GDP, of threonine in position 31 with asparagine (T31N) for ARFB1aGDP. The threonine in position 31 was exchanged with asparagine (T31N) to get ARFB1bGDP and of threonine in position 31 with asparagine (T31N) to get ARFB1cGDP.

To create the GTP-bound form, in the same way as for the GDP mutants, overlapping PCRs were done by substituting the glutamine at position 71 with the leucine (Q71L) to obtain ARF1GTP. The glutamine in position 71 was changed with the leucine for ARFB1aGTP, ARFB1bGTP, and for ARFB1cGTP. The coding sequence for ARFs in the GDP and GTP forms were fused at the C-terminus of YFP or GFP coding sequence. The mutant forms localization was observed at the confocal microscope to understand whether the active or inactive forms were important for their localization. Furthermore, the mutants ARF1GDP and GTP were coexpressed with the cargo molecule ERD2, since an influence of these mutants has been shown on the localization of this cargo (Stefano

et al., 2006). The other ARF mutants were coexpressed with SYP61, since a colocalization with this marker has been shown, and they could potentially change its localization.

ARF1GDP became completely cytosolic (Stefano et al., 2006), when overexpressed, it lost the capacity to bind to the Golgi apparatus and was mostly localized in the cytosol. In these conditions ERD2CFP relocalize to the ER (figure 3.9 panels A, B, and C). ARFB1aGDP did not loose its capability to bind to the plasma membrane, but it became more cytosolic (figure 3.9 panel D), ARFB1bGDP still localized at TGN level but was more cytosolic compared to its wild type form (figure 3.9 panel G). A similar result was found for ARFB1cGDP (figure 3.9 panel J). None of these constructs had influence on the localization of SYP61GFP, which continue to localize at TGN level (figure 3.9 panel E, H and K).

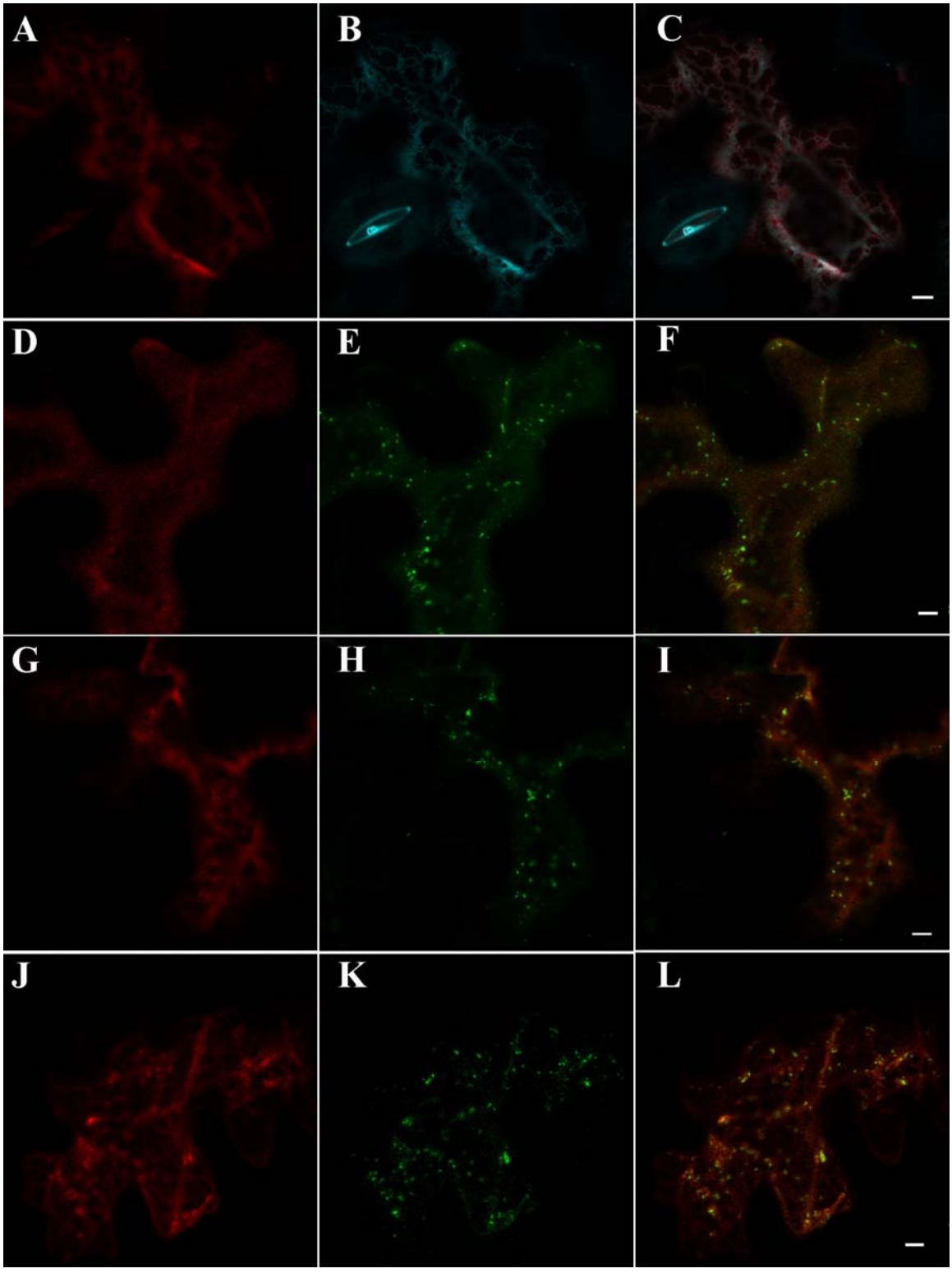
A
B
C
D
E
F
G
H
I
J
K
L

Fig 3.9: Subcellular localization of ARF1GDPYFP, ARFB1aGDPYFP, ARFB1bGDPYFP, ARFB1c YFPGDP and their influence on the localization of ERD2GFP and SYP61GFP.

Confocal images of tobacco leaf epidermal cells, 2 days after *A. tumefaciens* infiltration. ARF1GDPYFP (A) has a cytosolic localization. Its coexpression with ERD2CFP (B) causes ERD2 redistribution in the ER. ARFB1aGDPYFP (D), ARFB1bGDPYFP (G), ARFB1cGDPYFP (J) are more cytosolic then their wt forms but still define some punctate structures. The coexpression of these proteins in the GDP form with SYP61GFP (J), does not affect its localization. Panels C, F, I and L, are the respective merged images. Scale bars = 5 μm

The GTP form of ARF1 in low-level expression was still localizing at the Golgi apparatus, and coexpressed with ERD2GFP, the Golgi apparatus marker, does not affect its localization (figure 3.10, panels A, B and C).

For the others ARFs examined the GTP form was slightly more cytosolic compared to the wild type but the proteins did not loose their ability to bind to the membrane (figure 3.10, panels D, G and J). Furthermore, when the ARF proteins in their GTP form were coexpressed with SYP61, the TGN marker, they do not have any effect on its distribution (figure 3.10, panels E, H and K).

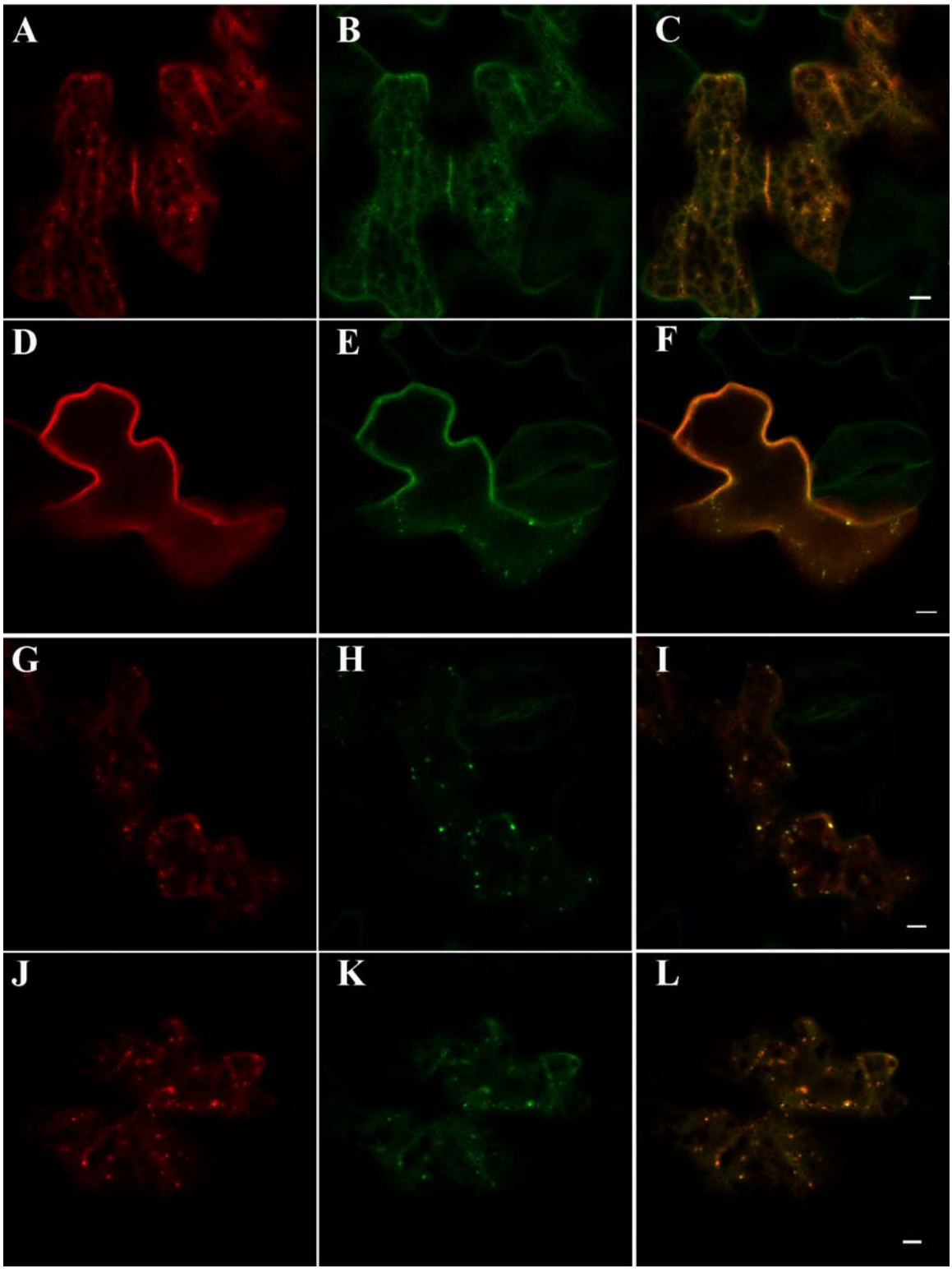
A
B
C
D
E
F
G
H
I
J
K
L

Fig 3.10: Subcellular localization of ARF1GTPYFP, ARFB1aGTPYFP, ARFB1bGTPYFP, ARFB1c GTPYFP, active forms and their influence on ERD2GFP and SYP61GFP localization.

Confocal images of tobacco leaf epidermal cells, 2 days after *A. tumefaciens* infiltration. ARF1GTPYFP (A) has a cytosolic localization. Its coexpression with ERD2GFP (B) causes not a strong effect on ERD2 redistribution. ARFB1aGTPYFP (D), ARFB1bGTPYFP (G), ARFB1cGTPYFP (J) became slightly more cytosolic but still localize at TGN level and extra post Golgi structures. When the ARFGTP mutants are coexpressed with SYP61GFP (J), they do not affect its localization. Panels C, F, I and L, are the respective merged images. Scale bars = 5 μm

3.5 BFA treatment

Protein recycling from the endosomes back to the PM is actin-dependent and sensitive to the fungal metabolite brefeldin A (BFA), an inhibitor of ARFGEFs (Donaldson et al., 1992; Helms and Rothman, 1992; Zeeh et al., 2006). ARF GTPases are important regulators involved in the development of secretory transport vesicles.

The use of this drug is an useful tool to investigate on the dynamic of the proteins involved in the transport from the ER to Golgi apparatus, which is regulated by ARF1 (Stefano et al., 2006).

To understand whether ARFB1a, ARFB1b, ARFB1c are BFA sensitive, a BFA treatment was done on transiently transformed leaves. This experiment was designed to understand whether the different ARFs are under the control of a BFA sensitive GEF. If this was not the case, ARFs with high similarity in sequence are under the control of different GEF. This could be a mechanism for an optimal pathogenesis response. Among the BFA sensitive ARFGEF in Arabidopsis there is the GNOM protein. GNOM is required for a correct targeting of PIN1, a protein required for the polarized auxin transport (Muday et

al., 2003). It has been shown in transgenic plants expressing the BFA resistant form of the GNOM, that also PIN1 trafficking and localization is BFA insensitive (Geldner et al., 2003). Several studies in plant cells reveal the existence of numerous recycling pathways for PM protein, which are regulated by distinct BFA-sensitive and BFA-resistant ARFGEFs. In case of a pathogen attack during which the pathogen releases the BFA compound in the cells, this system could permit the vesicle traffic notwithstanding the blockage of part of the pathway.

The treatment on ARF1YFP with BFA caused the redistribution of ARF1 into the cytosol as a control to test the efficacy of the treatment; the sample was cotransformed with ERD2, which in presence of BFA is redistributed to the ER (figure 3.11, panels A, B and C). The treatment on ARFB1aYFP demonstrates a more cytosolic distribution of the protein, even though the drug does not affect it localization at the plasma membrane (figure 3.11, panels D, E and F).

ARFB1bYFP BFA treatment resulted in a redistribution of the protein in the cytosol and only few of the punctuate structure originally marked persisted, probably due to an incomplete effect of the drug. Indeed in the same sample and also in ERD2, few of the Golgi bodies were still visible (figure 3.11, panels G, H and I). The same result was obtained for ARFB1cYFP treatment (figure 3.11, panels J, K and L) demonstrating that these ARFs are under the control of a BFA sensitive ARFGEF.

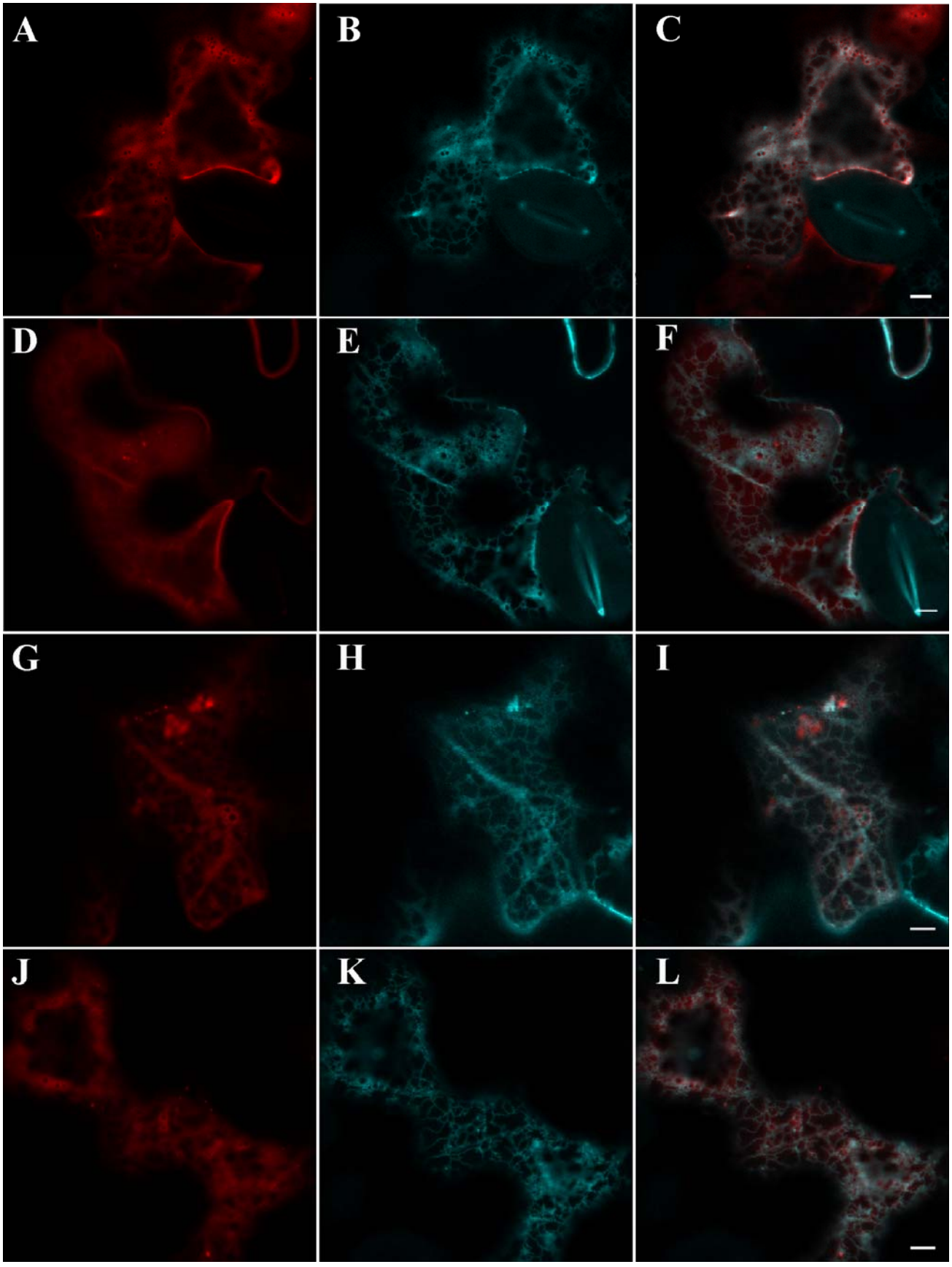
A
B
C
D
E
F
G
H
I
J
K
L

Fig 3.11: BFA sensitivity of ARF1YFP, ARFB1aYFP, ARFB1bYFP, ARFB1cYFP.

Confocal images of tobacco leaf epidermal cells, 2 days after *A. tumefaciens* infiltration after 1 hour incubation with BFA. ARF1YFP (A), ARFB1aYFP (D), ARFB1bYFP (G), and ARFB1cYFP (J) coexpressed with ERD2CFP (B, E, H, K), for all the constructs is possible to observe a relocalization in the cytosol after the incubation with BFA. ERD2CFP serves as control of the drug functionality. Scale bars = 5 μm

3.6 Kinetic analysis of ARF1, ARFB1a, ARFB1b, ARFB1c wild type and GTP forms

ARFs are highly dynamic in cell since it is known that ARFs peripherally and transitorily associates with membranes. In mammalian cells and plant cells, ARF1 has been shown to rapidly cycle between membranes and cytosol (Vasudevan et al., 1998; Stefano et al., 2006) but the membrane dynamics of other ARF members are unknown.

To study the binding of ARF proteins in living cells, we monitored the intracellular dynamics of ARFsGFP fusion proteins by FRAP (fluorescence recovery after photobleaching). In FRAP experiments; an intense laser pulse is used to irreversibly bleach the emission of light from a fluorescent molecule (e.g., GFP). Within the bleached area, the rate of fluorescence recovery (which is due to influx of unbleached area) is monitored by time lapse microscopy. The rationale for FRAP is that fluorescence recovery kinetics reflect the overall mobility of a protein (Carrero et al., 2004; Sprague and McNally, 2005). The ARFs GFP fusions ARF1, ARFB1a, ARFB1b, and ARFB1c, were transiently expressed in tobacco leaf epidermal cells, and the FRAP analysis was

conducted on a cortical section of tobacco leaf epidermal cells expressing the fluorescent constructs, by CLSM (confocal laser spectral microscopy).

The samples were treated with the drug latrunculin B, which having a negative effects on actin polymerization, stops the movement of all the structures having an actin dependent movement like the Golgi (Spector et al., 1983; Matheson et al., 2007).

After determining the initial fluorescence, a short laser pulse bleached the light emission of the GFP fusion protein within a small area of the cell. Then, the fluorescence recovery was monitored in short time intervals, revealing the recovery time, which is defined as the time after bleaching required for the fluorescence intensity to reach a constant value (Sprague and McNally, 2005). From the recovery curve, the time required to reach half maximal recovery time (t1/2) and the mobile fraction of the protein (Mf) can be determined (fig 2.2).

Furthermore, the dynamics of the proteins in their wild type form was compared to the kinetic of the GTP form.

FRAP analysis on ARF1YFP wt, confirms the data already obtained by Stefano and collaborators (Stefano et al., 2006), indeed the half maximal recovery time of 10.9± 1.5 s (seconds) (fig 3.12, panels A and B), while its GTP form takes a longer time that correspond to 19± 3.0 s (fig 3.12 panels C and D).

For ARFB1aYFPwt we measured has a half maximal recovery time of 16± 1.4 s (fig 3.13, panels A and B), while for ARFB1aGTPYFP it was 33.6± 3.2 s (fig 3.13, panels C and D).

FRAP analysis on ARFB1bYFPwt has a half maximal recovery time 12.2± 2.6 s (fig 3.14, panel A and B), and the ARFB1bGTPYFP it was 16.3± 2.8 s (fig 3.14, panel C and D).

For ARFB1cYFPwt the half maximal recovery time is 12.6± 1.5 s (fig 3.15, panels A and B) while its GTP form it is 24.3± 4.2 s (fig 3.15, panel C and D).

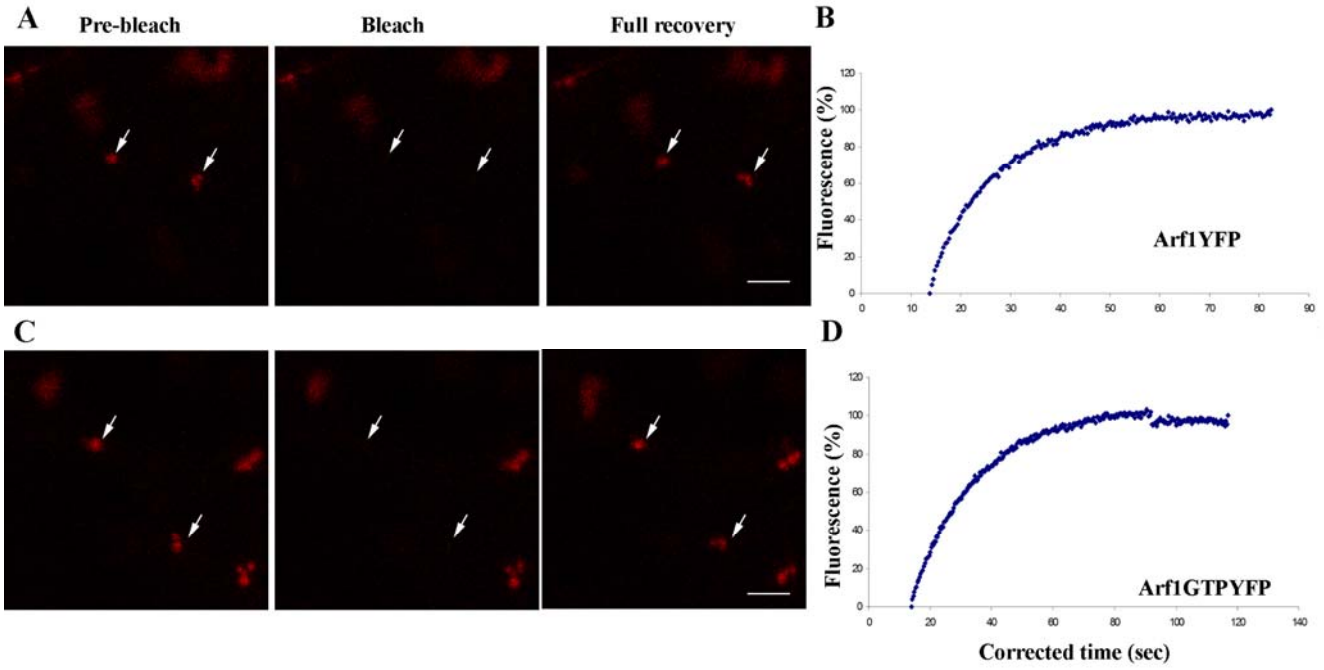

Fig 3.12: FRAP analysis on ARF1wtYFP and ARF1GTPYFP.

Panel A represents from the left to the right in order the pre-bleaching, bleaching and full recovery of Arf1wtYFP. The arrows indicate the regions that were bleached. B represents the corresponding graph indicating the half-time recovery curve of the fluorescence in cells expressing ARF1wtYFP (10.9± 1.5 s, n=20).

Panel C represents in order from the left to the right the pre-bleaching, bleaching and full recovery of ARF1GTP YFP. D represents the corresponding graph indicating the half-time recovery curve of the fluorescence in cells expressing ARF1GTPYFP (19± 3.0 s, n=20). Scale bars 5μm

Half time is defined as the time required for the fluorescence in the photobleached region to recover to 50% of the recovery asymptote and n represents the number of the bleached regions or organelles

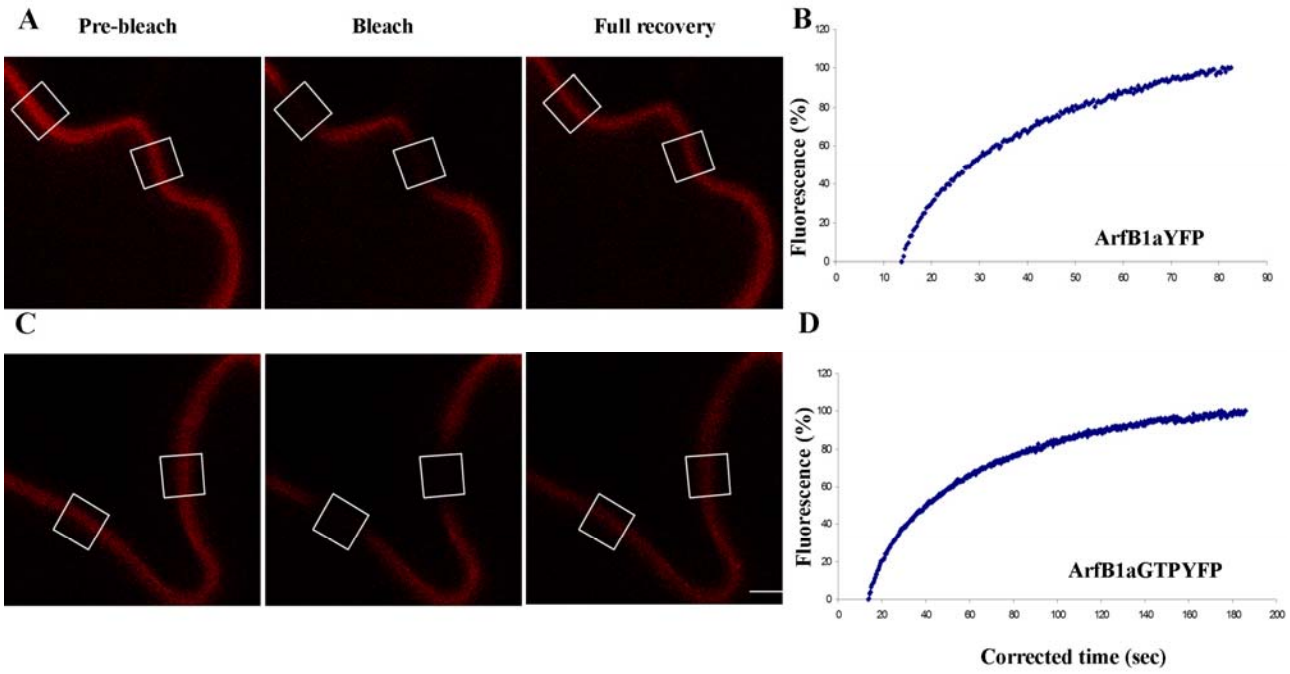

Fig 3.13: FRAP analysis on ARFB1awtYFP and ARFB1aGTPYFP.

Panel A represents from the left to the right in order the pre-bleaching, bleaching and full recovery of ARFB1awtYFP. The squares indicate the regions that were bleached. B represents the corresponding graph indicating the half-time recovery curve of the fluorescence in cells expressing ARFB1awtYFP (16± 1.4 s, n=20).

Panel C represents from the left to the right in order the pre-bleaching, bleaching and full recovery of ARFB1aGTPYFP. D represents the corresponding graph indicating the half-time recovery curve of the fluorescence in cells expressing ARFB1aGTPYFP (33.6± 3.2 s, n=20). Scale bars 5µm

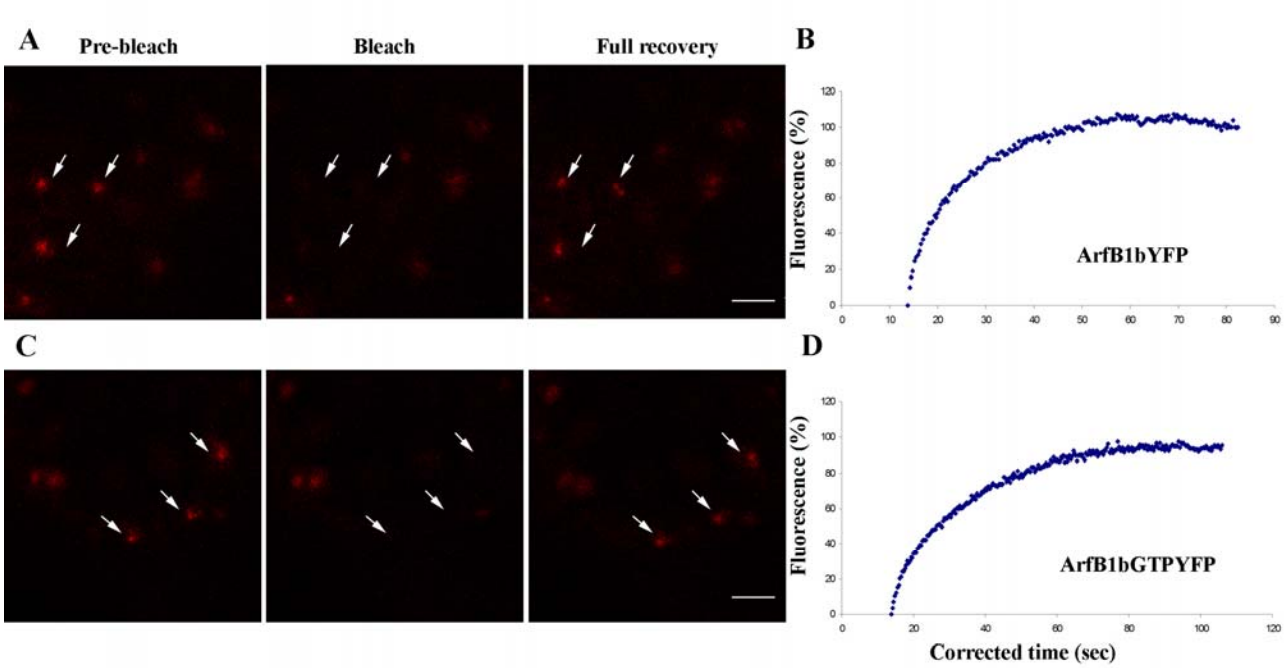

Fig 3.14: FRAP analysis on ARFB1bwtYFP and ARFB1bGTPYFP.

Panel A represents from the left to the right in order the pre-bleaching, bleaching and full recovery of ARFB1bwtYFP. The arrows indicate the regions that were bleached. B represents the corresponding graph indicating the half-time recovery curve of the fluorescence in cells expressing ARFB1bwtYFP (12.2± 2.6s, n=20).

Panel C represents in order, from the left to the right the pre-bleaching, bleaching and full recovery of ARFB1bGTPYFP. D represents the correspondent graph indicating the half-time recovery curve of the fluorescence in cells expressing ARFB1bGTPYFP (16.3± 2.8 s, n=20). Scale bars 5µm

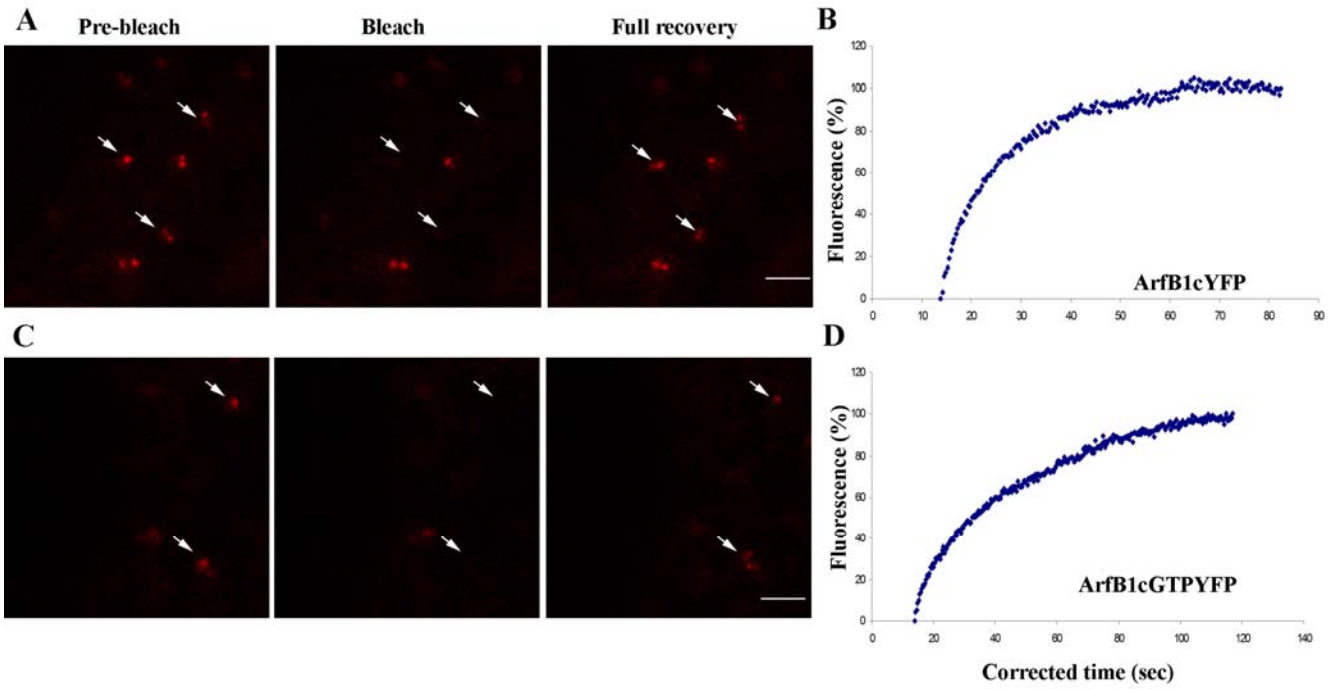

Fig 3.15: FRAP analysis on ARFB1cwtYFP and ARFB1cGTPYFP.

Panel A represents in order, from the left to the right the pre-bleaching, bleaching and full recovery of ARFB1cwtYFP. The arrows indicate the regions that were bleached. B represent the corresponding graph indicating the half-time recovery curves of the fluorescence in cells expressing ARFB1cwtYFP (12.6± 1.5 s, n=20).

Panel C represents in order, from the left to the right the pre-bleaching, bleaching and full recovery of ARFB1cGTPYFP. D represents the corresponding graph indicating the half-time recovery curve of the fluorescence in cells expressing ArfB1c GTPYFP (24.3± 4.2 s, n=20). Scale bars 5µm

In general all the different ARF proteins display different dynamic, the GTP forms of the proteins proved to display a mobility that is remarkably lower than that of the wt. The data obtained from the FRAP experiments are summarized in Table 1.
The comparison of the data between wt and GTP forms indicates anyhow recycling of the GTP, this means that the GTP mutants ability to recycle is not completely abolished.

Table 1: Mobility of YFP fusion proteins as determined by FRAP.

FUSION PROTEIN	**T1/2 (seconds)**
ARF1WtYFP	10.9± 1.5 s
ARF1GTPYFP	19± 3.0 s
ARFB1aWtYFP	16± 1.4 s
ARFB1aGTPYFP	33.6± 3.2 s
ARFB1bWtYFP	12.2± 2.6 s
ARFB1bGTPYFP	16.3± 2.8 s
ARFB1cWtYFP	12.6± 1.5 s
ARFB1cGTPYFP	24.3± 4.2 s

3.7 Impact on the secretory pathway of ARF1, ARFB1a, ARFB1b, ARFB1c wild type and GDP forms

In the previous chapters, it has been shown that these proteins might be involved in the secretory pathway.

To investigate the role for ARFB1a, ARFB1b, and ARFB1c in the secretion process, a biochemical test was applied. This test is based on the evaluation of the Rat preputial β-glucuronidase (SecRGUS) enzyme activity inside of the cells or outside of the cells. This enzyme is a useful marker to monitor the secretory trend of plant cells, first of all because its modified variant used for this experiment is efficiently secreted from the lumen of the ER via the Golgi complex toward the cell surface (Denecke et al., 1990; Leucci et al., 2007), second because is not a plant protein, so it is easy to quantify and to follow the inserted marker since there is not an endogenous one.

Tobacco protoplasts where transiently transformed with the following plasmids: SecRGUS alone (control), SecRGUS and ARF1wtYFP, SecRGUS and ARFB1awtYFP, SecRGUS and ARFB1bwtYFP, SecRGUS and ARFB1cwtYFP. As additional control it was used the GDP mutant of ARF1 which is known to hamper the secretion (Stefano et al., 2006). To check whether also the other ARFs protein in the GDP form have the same inhibitory effect on the secretion, protoplasts were also transformed with SecRGUS and ARFB1aGDPYFP, SecRGUS and ARFB1bGDPYFP, SecRGUS and ARFB1cGDPYFP. Twenty four hours later the protoplasts transient transformation, the SecRGUS secretion index in the medium and in the intracellular fraction was estimated. To quantify the SecRGUS activity the 4-methilumbelliferyl β-D-glucuronide was used as substrate.

An eventual intracellular enzyme contamination due to a possible break of the cells during the experimental procedure was evaluated measuring the α-mannosidase activity. The α-mannosidase is a plant cell enzyme which is not secreted. As substrate for the α-mannosidase activity measure, the 4-methilumbelliferyl α-D-mannopyranoside was used. The results were represented by a graph (fig. 3.16) reporting the secretion index relative to each transformation. The secretion index represents the ratio of extracellular and intracellular activities, and is expressed in arbitrary units. This test revealed that the wild type forms of the examined ARFs have a different impact on the secretion. The higher secretion index was found in protoplasts transformed with ARFB1bYFP; in particular it seems to stimulate the secretion (fig.3.16). ARF1YFP and ArfB1aYFP have comparable effects on the secretion, while ARFB1c seem to not greatly alter the normal secretion of the enzyme.

The GDP forms of the examined ARFs show in general an inhibitory effect compared to the wt forms. For some of them the inhibitory effect is stronger like for ARFB1aGDP, and for some of them it is less strong like for ARF1GDP. ARFB1bGDP and ARFB1cGDP have also inhibitory effect but ARFB1bGDP an effect on secretion seems to be lightly stronger then ARFB1cGDP.

In general the different impact on the secretion that has been found for the different wt and GDP mutant proteins would means that probably these proteins are involved in the regulation of different secretory routes or probably they control the pathway at different levels.

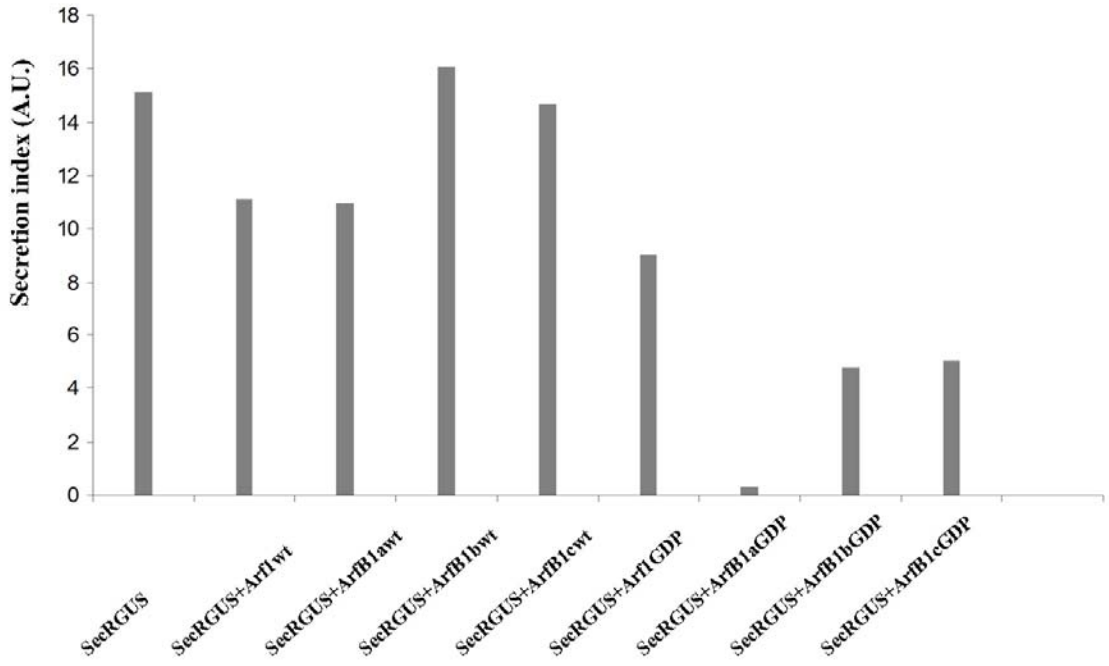

Fig 3.16: Secretion index for ARF1, ARFB1a, ARFB1b, ARFB1c.

SecRGUS secretion index for protoplasts samples transiently transformed with SecRGUS alone or in combination with ARF1wt, ARFB1awt, ARFB1bwt, ARFB1cwt, ARF1GDP, ARFB1aGDP, ARFB1bGDP, and ARFB1cGDP. Secretion index is calculated by the ratio of extracellular and intracellular activities and it is expressed in arbitrary units.

4.0 DISCUSSION

4.1 ARFB1b and ARFB1c localize at post Golgi structures

The endocytic machinery is a complex and important mechanism, which is still poorly characterized in plants. A very important role in the endocytosis process is held by some members of the small GTPases superfamilies like RAB and ARF, which are involved in membrane trafficking. The difference between these two kinds of proteins is that while RAB proteins are involved in a single trafficking step, ARFs are involved in multiple trafficking steps. This feature makes the ARFs a component of the secretory pathway that can offer much information in the study of the endocytic machinery. Furthermore, has been established, for only few of the 12 identified ARFs, an explicit function in the endocytic pathway. It has been shown that a particular motif identified in ARF1, MxxE, is responsible for the localization of the protein at Golgi apparatus (Matheson et al., 2008), while ARFB1a which has an IxxD motif in the same positions localizes to the plasma membrane and post Golgi apparatus structures.

Using bioinformatics tools other two ARFs proteins ARFB1b and ARFB1c, have been selected because of the presence of a motif, in the same region similar to IxxD. An additional DPF motif, important in human for the interaction with the AP2 complex, has been identified in the two selected ARFs. The presence of this additional motif also suggests the involvement of these proteins in the endocytic route.

Coexpression experiments of the GFP tagged ARFs with ERD2, the marker for the Golgi apparatus , the TGN marker SYP61, the marker of the early and late endosome FYVE construct and ARA7, and the PVC marker RHAI, demonstrated a localization of both

ARFB1b and ARFB1c on the TGN. This first result is very important since these proteins were completely unknown and nobody seems to have done an *in vivo* localization of them. Furthermore the localization of these two novel ARF proteins on the TGN led to the hypothesis that they might have an involvement in the machinery controlling the post-Golgi apparatus traffics. This hypothesis is corroborated by partial colocalization of ARFB1c with the two markers of early and late endosomes.

Several studies define the PVC and the late endosome as overlapping structure (Tse et al., 2004; Hanton et al., 2007). From the result obtained in the ARFB1c colocalization experiment, this protein partially colocalizes with FYVE and ARA7 (both early and late endosome markers) but not with RHAI (PVC marker). This result would mean that ARFB1c is only on the early endosome (if we assume that PVC and late endosome overlap). Alternatively, late endosome and PVC may be two separate structures. Cross cotransformation of the two `novel` ARFs (ARFB1b and ARFB1c) with ARF1 and ARFB1a revealed colocalization of these proteins at TGN level. The contemporaneous presence of different ARFs protein at the TGN is obviously a sign of a very active traffic at the TGN since it is the only compartment where secretory and endocytic pathways in plants intersect (Lam et al., 2007a).

One of the more recent hypotheses is that the TGN could contain distinct sorting domains (Koizumi et al., 2005) (fig 4.1); some of these domains are dedicated for synthesized proteins and recycling receptors traffic from the Golgi apparatus to the PM; some of them address traffic to the vacuole, and others to the endosome.

The results obtained in this thesis uphold this hypothesis and could be the key to clarify the functionality of all the mechanisms involved in TGN protein import/export.

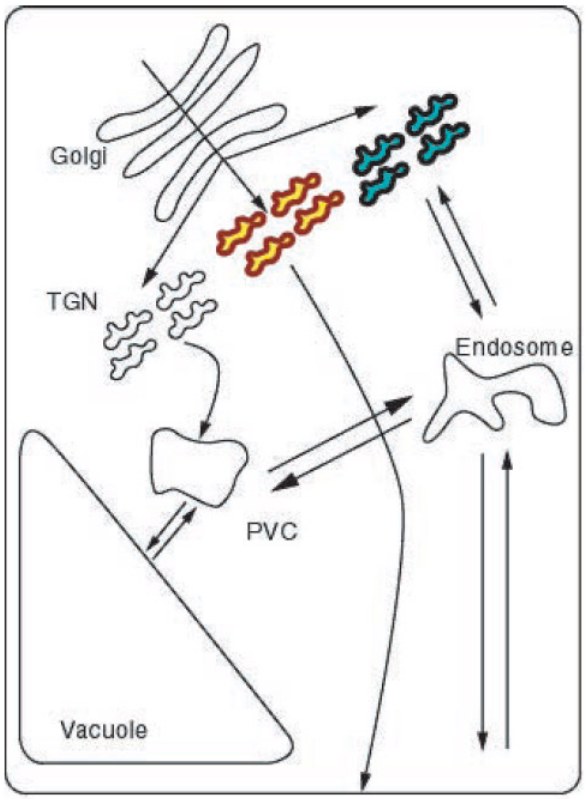

Fig 4.1: TGN functional differentiation.

In the picture are represented the TGN subpopulation, each subpopulation specific for a particular transport. The white subpopulation is for cargo transport to the PVC, the yellow one for transport to the plasma membrane, and the blue one for transport to the endosome. Picture from Koizumi et al 2005.

4.2 ARFB1b and ARFB1c are under the control of a BFA sensitive ARFGEF

ARF proteins localize to a extensive variety of membrane compartments, controlling different trafficking processes, playing a role in the recruitment of vesicle coats necessary for vesicle budding and cargo selection (Donaldson and Jackson, 2000).

ARF proteins exist in inactive GDP-bound and active GTP bound states. ARF activation leads to recruitment of coat proteins and lipid-modifying enzymes that in turn regulate the protein sorting and membrane deformation events associated with a given trafficking step (Nie et al., 2003). ARF activation is carried out by guanine nucleotide exchange factors ARFGEFs, which encode a GDP/GTP exchange factor for ARF proteins. In this way, ARFGEFs regulate vesicle formation in time and space by activating ARF substrates on distinct donor membranes, and confer specificity to ARF action (Donaldson and Jackson, 2000).

ARFGEFs are the molecular targets for the fungal toxin brefeldin A (BFA), which causes reversible inhibition of vesicle trafficking. BFA traps sensitive ARFGEFs on the membrane by hampering the guanine-nucleotide exchange reaction.

The total network and the structural changes of the endomembrane system of a BFA treated cell depends on the contribution of BFA-sensitive versus BFA-resistant ARFGEFs to the membrane traffic.

It is known that transcytosis in general and endosomes are structurally affected by BFA (Hunziker et al., 1991; Lippincott-Schwartz et al., 1991).

Compared to mammals, Arabidopsis has a higher number of BFA-sensitive ARFGEFs and only three out of the eight Arabidopsis ARFGEFs can be predicted to be BFA resistant.

Our finding shows that ARFB1b and ARFB1c are BFA sensitive, which means that they are likely regulated by a BFA sensitive ARFGEF.

The approach we used proved useful to investigate *in vivo* endomembrane activities for the novel ARF protein examined and supports our first observation on the involvement of these proteins on endosomal trafficking in plants.

4.3 Kinetic analysis

ARFGTPase proteins switch from the GDP inactivated state, in which they are free in the cytosol, to the GTP active state in which they are recruited and bind to the membrane of the organelle in which they carry out their specific function (Memon, 2004). This means that Arf proteins are normally not permanently bound to the membrane but they continuously pass from a cytosolic to a membrane-bound state and vice versa and this cycle is necessary to perform their activities.

Kinetic studies for ARFB1b and ARFB1c by FRAP analysis revealed a different half maximal recovery time (recovery rate) on the membrane.

The different recovery rates found for ARFB1b and ARFB1c indicates that the two proteins notwithstanding a very similar structure and conserved sequence have a different kinetics and could also have a different function. This observation is important because it is believed that many of the ARF isoforms are functionally redundant. By comparing the kinetic of ARFB1b and ARFB1c with the kinetic of ARF1 and ARFB1a, it was observed that ARF1 cycle very quickly on the membrane, and this confirm its multiple role in the secretory pathway both on the ER to Golgi apparatus transport and in the post Golgi apparatus traffic. Its speed is probably because it has to regulate active cargo traffic maintaining at the same time equilibrium inside the cell. ARFB1a has slower recovery rate, it is located on the plasma membrane, and probably there, it is easier to maintain

equilibrium since the traffic is probably less active. The others two ARFs: ARFB1b and ARFB1c have a kinetic more similar to ARF1; this can be explained by the fact that they are on the TGN, which is the junction point between the secretory and endocytic pathway, where it is possible to imagine the presence of a very active traffic, and the stability of the membranes have to be preserved.

The half-time recoveries analysis of the GTP-locked form of the ARFs analyzed shows that the GTP form is generally much slower than the wt forms. Furthermore, the slower recovery of the GTP form demonstrates that the GTP-locked forms are still able to recycle in part.

Taken together all these results suggest that ARFB1b and ARFB1c have a precise kinetic which depend on their specific activity at membrane level.

4.4 Impact of ARFB1b and ARFB1c on the secretory pathway

Proteins and glycoproteins directed to the vacuoles, to plasma membrane or to endosome move by vesicles trough the endomembrane system using conserved mechanisms (Northcote, 1979; Vitale and Denecke, 1999; Hanton et al., 2006).

It was recently demonstrated that in tobacco cells, different kinds of cargo, like cell wall polysaccharides and proteins reach the plasma membrane via different pathways (Leucci et al., 2007; Foresti and Denecke, 2008).

To understand the influence and the role of the secretion mechanism of ARFB1b and ARFB1c, these proteins were expressed in tobacco leaf protoplasts, and their effect on secretion was monitored by following the secretion index of a secreted glucuronidase, SecRGUS, that functions as secretory reporter protein (Leucci et al., 2007).

The SecRGUS secretion index measured in tobacco protoplasts transformed with ARFB1b and ARFB1c, showed different results leading to the hypothesis that the two proteins do not regulate the same pathway. It was in fact demonstrated that while ARFB1b stimulate the secretion, ARFB1c does not influence the normal secretion of the marker.

The same approach was used transforming protoplasts with a mutant form of the ARF proteins blocked in the GDP state. In this state the ARF proteins should be present in the cytosol, and not anymore on the membrane as required for cargo export. In this situation, if the mutated ARF protein is fundamental for the secretion of the secretory reporter protein, we should observe an important decrease of the secretion index. On the contrary, if the mutated ARF protein is not involved in the secretory process, the secretion index of the secretory reporter protein should be unaffected.

A different secretion index was found in presence of the GDP-locked form of these two proteins, in fact ARFB1bGDP and ARFB1cGDP inhibit the secretion more than ARF1GDP does, and in particular ARFB1cGDP reduce the secretion slightly less than ARFB1bGDP. ARFB1aGDP, drastically reduce the secretion index; this suggests it is located on the plasma membrane and its inactivity probably reduces dramatically the secretion.

The hypothesis arising from all these observations is that the two proteins (ARFB1bGDP and ARFB1cGDP) are involved in the regulation of a secretory pathway that is no less important during the secretion process than ARF1. It is known that ARF1GDP hampers the secretion (Stefano et al., 2006), but the finding that ARFB1bGDP and ARFB1cGDP hamper the secretion slightly more than ARF1GDP, suggests that they may have a very

strong effect in the post Golgi traffic, from the TGN on the way out of the cell. Moreover, since the effects of ARFB1bGDP and ARFB1cGDP on secretion are not exactly the same, it is possible to imagine that they are involved in two different pathways especially, since the GDP-locked form for ARFB1b and ARFB1c have noticeable but slightly different inhibitory effect on secretion. Combining the data collected from the confocal microscopy analysis with the secretory test results it is possible to imagine that ARFB1b, which is located on TGN, regulates the traffic to the plasma membrane. Instead is possible to explain the influence on the secretion of ARFB1c, which is located on TGN and early/late endosome, deducing that this protein regulates the traffic to a different post Golgi compartment as could be the endosomes. This hypothesis fits perfectly with the result obtained by confocal microscopy analysis. To explain the incomplete inhibition of ARFB1bGDP and ARFB1cGDP form it is possible to suppose that when one of the pathways is blocked, in some way a parallel pathway is stimulated and activated the secretion to the plasma membrane, and to avoid the endomembrane system collapse. This idea supports the existence of a balancing mechanism, which acts to maintain the stability and the integrity of the endomembrane system.

4.5 Concluding remarks

In plant cells, ARFs represent an important family of proteins that have multiple activities essential to the function of the secretory pathway (Matheson et al., 2007). These proteins regulate complex protein-protein interactions (Matheson et al., 2008), regulate responses to pathogenesis and are implicated in the maintenance of organelle structure (Memon, 2004). A few reports show the ARFs are also involved in the still unexplored endocytic

machinery in plants. However, due to the high similarity and complexity of the ARF family, for most of the identified ARFs functions have not yet been assigned (Lee and Sano, 2007).

The results gained in this thesis represent an improvement in the knowledge of ARF GTPases and their role in the endocytic machinery.

Two previously uncharacterized ARF proteins have been identified by following the presence of specific motifs, which dictates protein localization.

It has been demonstrated that these motifs are conserved across the eukaryotes kingdom indeed the IxxD motif that we take in consideration for the identification of new proteins, is conserved and is similar in human (Honda et al., 2005). In addition, the presence of an additional DPF motif that in human is important for the interaction with the AP2 complex (Brett et al., 2002a) suggests a conserved function of this motif in plant cells.

It has been demonstrated that all ARF protein homologues do not have redundant functions. On the contrary, they have their own functionality. This was confirmed by their different localization pattern, different kinetics and different effects on the secretory pathway.

ARFB1b and ARFB1c, two ARFs homologues, were shown to be located in post Golgi compartment known as the TGN, which is involved in the endocytic machinery.

Further experiments to evaluate their kinetic and secretion influence in presence of specific cargo molecules could help to understand whether they regulate a determinate kind of cargo and reveal more details on their mechanisms of action.

5. APPENDIX A

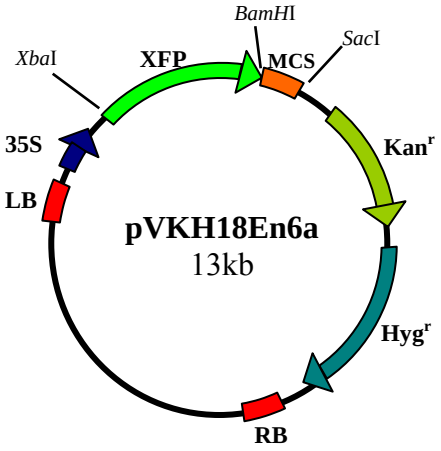

Figure A1. Schematic structure of pVKH18En6a which carries the kanamycin resistance (Kan^r in bacteria), hygromycin resistance (Hyg^r in plants), the multiple cloning site (MCS), gene encoding for fluorescent protein (XFP) (X = green, cyan or yellow) at the N-terminal of MCS, the 35S promoter, the left border (LB) and right border (RB) flanking the T-DNA.

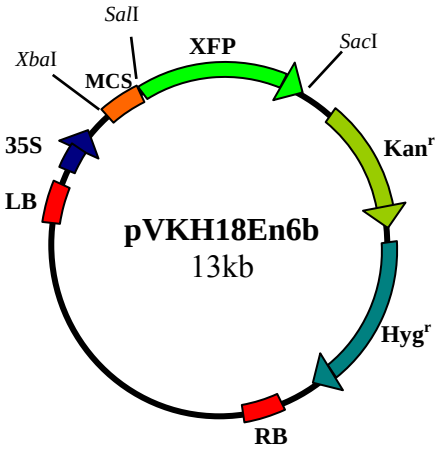

Figure A2. Schematic structure of pVKH18En6b which carries the kanamycin resistance (Kan^r in bacteria), hygromycin resistance (Hyg^r in plants), the multiple cloning site (MCS), gene encoding for green fluorescent protein (XFP) (X = green, cyan or yellow) at the C-terminal of MCS, the 35S promoter, the left border (LB) and right border (RB) flanking the T-DNA.

Table A1. Plasmids, *Agrobacterium tumefaciens* and *E. coli* strains used in this work.

Plasmids	resistance
pVKH18EN6a[c]	Kanamycin^R, Hygromycin^R
pVKH18EN6b[c]	Kanamycin^R , Hygromycin^R
Agrobacterium tumefaciens strain	
GV3101[d]	Gentamycin^R
Escherichia coli strains	
MC1061[e]	Streptomycin^R

(a) Novagen (www.novagen.com), (b) (Kaelin et al., 1992), (c) (Batoko et al., 2000), (d) Brandizzi lab's stock, (e) Invitrogen (www.invitrogen.com), (f) Stratagene (www.stratagene.com).

Table A2. Solutions. All the solutions were prepared as in (a) QIAGEN-QIAexpressionist; (b) Sambrook et al., 1989; (c) Thorpe and Kricka, 1986; (d) BD biosciences, glutathione resins user manual; (e) Lu and Hong, 2003.

Solutions	**Fomulations**
Sample buffer 5X [a]	0.225 M Tris-HCl, pH 6.8; 50 % glycerol; 5 % SDS; 0.05 % bromophenol blue; 0.25 M DTT
TFBI [b]	30 mM $KC_2H_3O_2$, 100 mM RbCl, 10 mM $CaCl_2$-$2H_2O$, 50 mM MnCl2-4H2O, 15 % glycerol, pH 5.8 with 0.2 M CH3COOH.
TFBII [b]	10 mM MOPS, 10 mM RbCl, 75 mM $CaCl_2$-$2H_2O$, 15 % glycerol, pH 6.6 with 1M KOH.
50X TAE [b]	242 g/l Tris base, 57.1 ml/l glacial acetic acid, 37.2 $Na_2EDTA2H_2O$
Loading buffer 10X [b]	35 % glycerol, 2.5 g/l Bromophenol blue in 10 X TAE
P1 [a]	1 mM EDTA, 50 mM TRIS, pH 8.0.
P2 [a]	0.2 N NaOH, 1 % SDS.
P3 [a]	11.5 % acetic acid, 3 M potassium acetate, pH 5.5.

Solutions	**Fomulations**
Washing solution [b]	136.9 g/l sucrose (0.4M), 2.4 g/l Hepes, 6 g/l KCl, 600 mg/l CaCl2×2H2O, pH7.2 (with KOH)
TEX Buffer	3.1 g/l Gamborg`s B5 Salts (Sigma), 500 mg/l MES, 750 mg/l CaCl2×2H2O, 250 mg/l NH4NO3, 136.9 g/l sucrose (0.4M), pH5.7 (with 1M KOH)
10X leaf digestion mix	2% w/v macerozyme R-10, 4%w/v cellulase R-10 in TEX buffer
PEG solution	40% PEG4000, 0.4M mannitol, 0.1M Ca(NO3)2×4H2O, pH8 with 0.5M KOH
MMM solution	0.5M Mannitol, 15mM MgCl2, 0.1% MES
10X PBS [b]	87 g/l NaCl, 22.5 g/l $Na_2HPO4\text{-}2H_2O$, 2 g/l KH_2PO_4, pH 7.4.
Kanamycin	Stock solution in water 100 mg/ml, kept at -20ºC.
Ampicillin	Stock solution in water 100 mg/ml, kept at -20ºC.
Gentamycin	Stock solution in water 100 mg/ml, kept at -20 º C.
IF	20 mM $Na_3(PO_4)$, 500 mM MES, 200 mM acetosyringone, 5 mg/ml glucose.

Table A3. Primers used in PCR reactions. All the primers were purchased from Invitrogen, desalted and with a scale of 50 nM.

Primer	**Sequence**	**Restriction site**	**Protein generated**
LR95F	CAGGACGTCTAGATGGGGTTGTCATTCGGAAAGTTGTTC	*XbaI*	ARF1
LR96F	CATGACCGTCGACTTTGCCTTGCTTGCGATGTTGTTGGA	*Sal*I	ARF1
LR97F	GCTGCTGGTAAGAACACTATCCTCTAC	n.a.	ARF1-GDP
LR98F	GTAGAGGATAGTGTTCTTACCAGCAGC	n.a.	ARF1-GDP
LR99F	GATGTTGGGGGTCTAGACAAGATCCGT	n.a.	ARF1-GTP
LR100F	ACGGATCTTGTCTAGACCCCCAACATC	n.a.	ARF1-GTP
LR33F	CAGGACGTCTAGATGGGA GCCAGATTTTCACGTATAG	*XbaI*	ARFB1a
LR34F	CATGACCGTCGACTTATACCTCGGACCTCGGACCAGCTT	*Sal*I	ARFB1a
LR35F	GGTTCAGGGAAGAATACCATCCTTTAC	n.a.	ARFB1a-GDP
LR36F	GTAAAGGATGGTATTCTTCCCTGAACC	n.a.	ARFB1a-GDP
LR37F	GATATAGGAGGACTAGAGAAG ATTCGC	n.a.	ARFB1a-GTP
LR38F	GCGAATCTTCTCTAGTCCTCCTATATC	n.a.	ARFB1a-GTP
LR39F	CAGGACGTCTAGATGGGTCAAGCTTTTCGTAAGCTA	*XbaI*	ARFB1b
LR40F	CATGACCGTCGACTTAAACGAGTGGCCAACCGATGTGAA	*Sal*I	ARFB1b
LR41F	GCTGCTGGAAAAAATACTATTCTCTAC	n.a.	ARFB1b-GDP
LR42F	GTAGAGAATAGTATTTTTTCCAGCAGC	n.a.	ARFB1b-GDP
LR43F	GAT GTTGGTGGCCTAGAGAAACTGAGA	n.a.	ARFB1b-GTP
LR44F	TCTCAGTTTCTCTAGGCCACCAACATC	n.a.	ARFB1b-GTP
LR45F	CAGGACGTCTAGATGGGTCAAACTTTTCGCAAGCTT	*XbaI*	ARFB1c
LR46F	CATGACCGTCGACTTAAACGAGGGACCAAC TGATGAG	*Sal*I	ARFB1c
LR47F	GCGGCTGGCAAAAATACGATACTATAC	n.a.	ARFB1c-GDP
LR48F	GTATAGTATCGTATTTTTGCCAGCCGC	n.a.	ARFB1c-GDP
LR49F	GATGTTGGTGGCCTAGAGAAGCTGAGG	n.a.	ARFB1c-GTP
LR50F	CCTCAGCTT CTCTAGGCCACCAACATC	n.a.	ARFB1c-GTP

(n.a.= non applicable because these are internal primers used for overlapping PCRs).

Table A4. Mutations produced using the overlapping PCR.

Mutations	**Primers used**	**cDNA used**	**Protein generated**	**Vector used**
T31N	LR97F	At2g47170	ARF1-GDP	PVKH18En6
	LR98F			
Q71L	LR99F		ARF1-GTP	PVKH18En6
	LR100F			
T31N	LR35F	At2g15310	ARFB1a-GDP	PVKH18En6
	LR36F			
Q71L	LR37F		ARFB1a-GTP	PVKH18En6
	LR38F			
T31N	LR41F	At5g17060	ARFB1b-GDP	PVKH18En6
	LR42F			
Q71L	LR43F		ARFB1b-GTP	PVKH18En6
	LR44F			
T31N	LR47F	At3g03120	ARFB1c-GDP	PVKH18En6
	LR48F			
Q71L	LR49F		ARFB1c-GTP	PVKH18En6
	LR50F			

Table A5. Media. All the media described were prepared as in Sambrook et al. (1989).

Medium	**Formulation**
LB liquid	10 g/l bacto peptone-tryptone, 5 g/l yeast extract, 10 g/l NaCl.
LB solid	10 g/l bacto peptone-tryptone, 5 g/l yeast extract, 10 g/l NaCl, 10 g/l agar.
YT	16 g/l bacto-tryptone, 10 g/l yeast extract, 5 g/l NaCl, pH 7.0.

Table A6. Composition of PCR reactions

Reagent	
Template DNA	1 µl
Pfu buffer (10x)+ $MgSO_4$(25 mM)	20 µl
Pfu DNA Polymerase (Fermentas)	1 µl
Sense primer (50 pmol/ µl)	0.6 µl
Antisense primer (50 pmol/ µl)	0.6 µl
dNTP (100 mM)	4 µl
Sterile distilled H_2O	172.8 µl

(Aliquoted in two tubes and overlaid with mineral oil).

6. REFERENCES

Barth, M., and Holstein, S.E. (2004). Identification and functional characterization of Arabidopsis AP180, a binding partner of plant alphaC-adaptin. J Cell Sci **117,** 2051-2062.

Batoko, H., Zheng, H.Q., Hawes, C., and Moore, I. (2000). A rab1 GTPase is required for transport between the endoplasmic reticulum and golgi apparatus and for normal golgi movement in plants. Plant Cell **12,** 2201-2218.

Beraud-Dufour, S., Paris, S., Chabre, M., and Antonny, B. (1999). Dual interaction of ADP ribosylation factor 1 with Sec7 domain and with lipid membranes during catalysis of guanine nucleotide exchange. J Biol Chem **274,** 37629-37636.

Bigay, J., Gounon, P., Robineau, S., and Antonny, B. (2003). Lipid packing sensed by ArfGAP1 couples COPI coat disassembly to membrane bilayer curvature. Nature **426,** 563-566.

Boevink, P., Oparka, K., Santa Cruz, S., Martin, B., Betteridge, A., and Hawes, C. (1998). Stacks on tracks: the plant Golgi apparatus traffics on an actin/ER network. Plant J **15,** 441-447.

Brandizzi, F., and Hawes, C. (2004). A long and winding road: symposium on membrane trafficking in plants. EMBO Rep **5,** 245-249.

Brandizzi, F., Frangne, N., Marc-Martin, S., Hawes, C., Neuhaus, J.M., and Paris, N. (2002). The destination for single-pass membrane proteins is influenced markedly by the length of the hydrophobic domain. Plant Cell **14,** 1077-1092.

Brett, C.L., Wei, Y., Donowitz, M., and Rao, R. (2002a). Human Na(+)/H(+) exchanger isoform 6 is found in recycling endosomes of cells, not in mitochondria. Am J Physiol Cell Physiol **282,** C1031-1041.

Brett, T.J., Traub, L.M., and Fremont, D.H. (2002b). Accessory protein recruitment motifs in clathrin-mediated endocytosis. Structure **10,** 797-809.

Carrero, G., Crawford, E., Hendzel, M.J., and de Vries, G. (2004). Characterizing fluorescence recovery curves for nuclear proteins undergoing binding events. Bull Math Biol **66,** 1515-1545.

daSilva, L.L., Snapp, E.L., Denecke, J., Lippincott-Schwartz, J., Hawes, C., and Brandizzi, F. (2004). Endoplasmic reticulum export sites and Golgi bodies behave as single mobile secretory units in plant cells. Plant Cell **16,** 1753-1771.

daSilva, L.L., Taylor, J.P., Hadlington, J.L., Hanton, S.L., Snowden, C.J., Fox, S.J., Foresti, O., Brandizzi, F., and Denecke, J. (2005). Receptor salvage from the prevacuolar compartment is essential for efficient vacuolar protein targeting. Plant Cell **17,** 132-148.

Denecke, J., Botterman, J., and Deblaere, R. (1990). Protein secretion in plant cells can occur via a default pathway. Plant Cell **2,** 51-59.

Dettmer, J., Hong-Hermesdorf, A., Stierhof, Y.D., and Schumacher, K. (2006). Vacuolar H+-ATPase activity is required for endocytic and secretory trafficking in Arabidopsis. Plant Cell **18,** 715-730.

Di Sansebastiano, G.P., Paris, N., Marc-Martin, S., and Neuhaus, J.M. (1998). Specific accumulation of GFP in a non-acidic vacuolar compartment via a C-terminal propeptide-mediated sorting pathway. Plant J **15,** 449-457.

Donaldson, J.G., and Jackson, C.L. (2000). Regulators and effectors of the ARF GTPases. Curr Opin Cell Biol **12,** 475-482.

Donaldson, J.G., Finazzi, D., and Klausner, R.D. (1992). Brefeldin A inhibits Golgi membrane-catalysed exchange of guanine nucleotide onto ARF protein. Nature **360,** 350-352.

Emans, N., Zimmermann, S., and Fischer, R. (2002). Uptake of a fluorescent marker in plant cells is sensitive to brefeldin A and wortmannin. Plant Cell **14,** 71-86.

Floyd, S., and De Camilli, P. (1998). Endocytosis proteins and cancer: a potential link? Trends Cell Biol **8,** 299-301.

Foresti, O., and Denecke, J. (2008). Intermediate organelles of the plant secretory pathway: identity and function. Traffic **9,** 1599-1612.

Foresti, O., daSilva, L.L., and Denecke, J. (2006). Overexpression of the Arabidopsis syntaxin PEP12/SYP21 inhibits transport from the prevacuolar compartment to the lytic vacuole in vivo. Plant Cell **18,** 2275-2293.

Gebbie, L.K., Burn, J.E., Hocart, C.H., and Williamson, R.E. (2005). Genes encoding ADP-ribosylation factors in Arabidopsis thaliana L. Heyn.; genome analysis and antisense suppression. J Exp Bot **56,** 1079-1091.

Geldner, N. (2004). The plant endosomal system--its structure and role in signal transduction and plant development. Planta **219,** 547-560.

Geldner, N., Anders, N., Wolters, H., Keicher, J., Kornberger, W., Muller, P., Delbarre, A., Ueda, T., Nakano, A., and Jurgens, G. (2003). The Arabidopsis GNOM ARF-GEF mediates endosomal recycling, auxin transport, and auxin-dependent plant growth. Cell **112,** 219-230.

Glick, B.S., and Malhotra, V. (1998). The curious status of the Golgi apparatus. Cell **95,** 883-889.

Griffith, G. (2000). Gut thoughts on the Golgi complex. Traffic **1,** 738-745.

Gruenberg, J. (2001). The endocytic pathway: a mosaic of domains. Nat Rev Mol Cell Biol **2,** 721-730.

Hadlington, J.L., and Denecke, J. (2000). Sorting of soluble proteins in the secretory pathway of plants. Curr Opin Plant Biol **3,** 461-468.

Hanton, S.L., Matheson, L.A., and Brandizzi, F. (2006). Seeking a way out: export of proteins from the plant endoplasmic reticulum. Trends Plant Sci **11,** 335-343.

Hanton, S.L., Matheson, L.A., Chatre, L., Rossi, M., and Brandizzi, F. (2007). Post-Golgi protein traffic in the plant secretory pathway. Plant Cell Rep **26,** 1431-1438.

Helms, J.B., and Rothman, J.E. (1992). Inhibition by brefeldin A of a Golgi membrane enzyme that catalyses exchange of guanine nucleotide bound to ARF. Nature **360,** 352-354.

Higuchi, R., Krummel, B., and Saiki, R.K. (1988). A general method of in vitro preparation and specific mutagenesis of DNA fragments: study of protein and DNA interactions. Nucleic Acids Res **16,** 7351-7367.

Hillmer, S., Movafeghi, A., Robinson, D.G., and Hinz, G. (2001). Vacuolar storage proteins are sorted in the cis-cisternae of the pea cotyledon Golgi apparatus. J Cell Biol **152,** 41-50.

Hinz, G., Hillmer, S., Baumer, M., and Hohl, I.I. (1999). Vacuolar storage proteins and the putative vacuolar sorting receptor BP-80 exit the golgi apparatus of developing pea cotyledons in different transport vesicles. Plant Cell **11,** 1509-1524.

Ho, S.N., Hunt, H.D., Horton, R.M., Pullen, J.K., and Pease, L.R. (1989). Site-directed mutagenesis by overlap extension using the polymerase chain reaction. Gene **77,** 51-59.

Holstein, S.E. (2002). Clathrin and plant endocytosis. Traffic **3,** 614-620.

Honda, A., Al-Awar, O.S., Hay, J.C., and Donaldson, J.G. (2005). Targeting of Arf-1 to the early Golgi by membrin, an ER-Golgi SNARE. J Cell Biol **168,** 1039-1051.

Hunziker, W., Whitney, J.A., and Mellman, I. (1991). Selective inhibition of transcytosis by brefeldin A in MDCK cells. Cell **67,** 617-627.

Hutter, H. (2004). Five-colour in vivo imaging of neurons in Caenorhabditis elegans. J Microsc **215,** 213-218.

Hyun, T.S., and Ross, T.S. (2004). HIP1: trafficking roles and regulation of tumorigenesis. Trends Mol Med **10,** 194-199.

Kaelin, W.G., Jr., Krek, W., Sellers, W.R., DeCaprio, J.A., Ajchenbaum, F., Fuchs, C.S., Chittenden, T., Li, Y., Farnham, P.J., Blanar, M.A., and et al. (1992). Expression cloning of a cDNA encoding a retinoblastoma-binding protein with E2F-like properties. Cell **70,** 351-364.

Kapila, J., De Rycke, R., Van Montagu, M., and Angenon, G. (1997). An Agrobacterium-mediated transient gene expression system for intact leaves. Plant Science **122,** 101-108.

Kirsch, T., Paris, N., Butler, J.M., Beevers, L., and Rogers, J.C. (1994). Purification and initial characterization of a potential plant vacuolar targeting receptor. Proc Natl Acad Sci U S A **91,** 3403-3407.

Klausner, R.D., Donaldson, J.G., and Lippincott-Schwartz, J. (1992). Brefeldin A: insights into the control of membrane traffic and organelle structure. J Cell Biol **116,** 1071-1080.

Koizumi, K., Naramoto, S., Sawa, S., Yahara, N., Ueda, T., Nakano, A., Sugiyama, M., and Fukuda, H. (2005). VAN3 ARF-GAP-mediated vesicle transport is involved in leaf vascular network formation. Development **132,** 1699-1711.

Lam, S.K., Tse, Y.C., Robinson, D.G., and Jiang, L. (2007a). Tracking down the elusive early endosome. Trends Plant Sci **12,** 497-505.

Lam, S.K., Siu, C.L., Hillmer, S., Jang, S., An, G., Robinson, D.G., and Jiang, L. (2007b). Rice SCAMP1 defines clathrin-coated, trans-golgi-located tubular-vesicular structures as an early endosome in tobacco BY-2 cells. Plant Cell **19,** 296-319.

Latijhouwerrs, M., Hawes, C., and Carvalho, C. (2005). Holding it all together? Candidate proteins for the plant Golgi matrix. Current opinion in Plant Biology **8,** 1-8.

Lee, G.J., Sohn, E.J., Lee, M.H., and Hwang, I. (2004). The Arabidopsis rab5 homologs rha1 and ara7 localize to the prevacuolar compartment. Plant Cell Physiol **45,** 1211-1220.

Lee, M.H., and Sano, H. (2007). Attenuation of the hypersensitive response by an ATPase associated with various cellular activities (AAA) protein through suppression of a small GTPase, ADP ribosylation factor, in tobacco plants. Plant J **51,** 127-139.

Lefebvre, B., Batoko, H., Duby, G., and Boutry, M. (2004). Targeting of a Nicotiana plumbaginifolia H+ -ATPase to the plasma membrane is not by default and requires cytosolic structural determinants. Plant Cell **16,** 1772-1789.

Leucci, M.R., Di Sansebastiano, G.P., Gigante, M., Dalessandro, G., and Piro, G. (2007). Secretion marker proteins and cell-wall polysaccharides move through different secretory pathways. Planta **225,** 1001-1017.

Lippincott-Schwartz, J., Roberts, T.H., and Hirschberg, K. (2000). Secretory protein trafficking and organelle dynamics in living cells. Annu Rev Cell Dev Biol **16,** 557-589.

Lippincott-Schwartz, J., Yuan, L., Tipper, C., Amherdt, M., Orci, L., and Klausner, R.D. (1991). Brefeldin A's effects on endosomes, lysosomes, and the TGN suggest a general mechanism for regulating organelle structure and membrane traffic. Cell **67,** 601-616.

Matheson, L.A., Suri, S.S., Hanton, S.L., Chatre, L., and Brandizzi, F. (2008). Correct targeting of plant ARF GTPases relies on distinct protein domains. Traffic **9,** 103-120.

Matheson, L.A., Hanton, S.L., Rossi, M., Latijnhouwers, M., Stefano, G., Renna, L., and Brandizzi, F. (2007). Multiple roles of ADP-ribosylation factor 1 in plant cells include spatially regulated recruitment of coatomer and elements of the Golgi matrix. Plant Physiol **143,** 1615-1627.

Meckel, T., Hurst, A.C., Thiel, G., and Homann, U. (2004). Endocytosis against high turgor: intact guard cells of Vicia faba constitutively endocytose fluorescently labelled plasma membrane and GFP-tagged K-channel KAT1. Plant J **39,** 182-193.

Memon, A.R. (2004). The role of ADP-ribosylation factor and SAR1 in vesicular trafficking in plants. Biochim Biophys Acta **1664,** 9-30.

Morise, H., Shimomura, O., Johnson, F.H., and Winant, J. (1974). Intermolecular energy transfer in the bioluminescent system of Aequorea. Biochemistry **13,** 2656-2662.

Mossessova, E., Corpina, R.A., and Goldberg, J. (2003). Crystal structure of ARF1*Sec7 complexed with Brefeldin A and its implications for the guanine nucleotide exchange mechanism. Mol Cell **12,** 1403-1411.

Muday, G.K., Peer, W.A., and Murphy, A.S. (2003). Vesicular cycling mechanisms that control auxin transport polarity. Trends Plant Sci **8,** 301-304.

Munro, S. (2002). Organelle identity and the targeting of peripheral membrane proteins. Curr Opin Cell Biol **14,** 506-514.

Munro, S. (2005). The Arf-like GTPase Arl1 and its role in membrane traffic. Biochem Soc Trans **33,** 601-605.

Murphy, A.S., Bandyopadhyay, A., Holstein, S.E., and Peer, W.A. (2005). Endocytotic cycling of PM proteins. Annu Rev Plant Biol **56,** 221-251.

Neumann, U., Brandizzi, F., and Hawes, C. (2003). Protein transport in plant cells: in and out of the Golgi. Ann Bot (Lond) **92,** 167-180.

Nie, Z., Hirsch, D.S., and Randazzo, P.A. (2003). Arf and its many interactors. Curr Opin Cell Biol **15,** 396-404.

Northcote, D.H. (1979). The involvement of the Golgi apparatus in the biosynthesis and secretion of glycoproteins and polysaccharides. Biomembranes **10,** 51-76.

Otegui, M.S., Herder, R., Schulze, J., Jung, R., and Staehelin, L.A. (2006). The proteolytic processing of seed storage proteins in Arabidopsis embryo cells starts in the multivesicular bodies. Plant Cell **18,** 2567-2581.

Ovecka, M., Lang, I., Baluska, F., Ismail, A., Illes, P., and Lichtscheidl, I.K. (2005). Endocytosis and vesicle trafficking during tip growth of root hairs. Protoplasma **226,** 39-54.

Palade, G. (1975). Intracellular aspects of the process of protein synthesis. Science **189,** 347-358.

Paris, N., and Neuhaus, J.M. (2002). BP-80 as a vacuolar sorting receptor. Plant Mol Biol **50,** 903-914.

Paris, N., Stanley, C.M., Jones, R.L., and Rogers, J.C. (1996). Plant cells contain two functionally distinct vacuolar compartments. Cell **85,** 563-572.

Pasqualato, S., Renault, L., and Cherfils, J. (2002). Arf, Arl, Arp and Sar proteins: a family of GTP-binding proteins with a structural device for 'front-back' communication. EMBO Rep **3,** 1035-1041.

Pimpl, P., Movafeghi, A., Coughlan, S., Denecke, J., Hillmer, S., and Robinson, D.G. (2000). In situ localization and in vitro induction of plant COPI-coated vesicles. Plant Cell **12,** 2219-2236.

Preuss, D., Mulholland, J., Franzusoff, A., Segev, N., and Botstein, D. (1992). Characterization of the Saccharomyces Golgi complex through the cell cycle by immunoelectron microscopy. Mol Biol Cell **3,** 789-803.

Raiborg, C., Rusten, T.E., and Stenmark, H. (2003). Protein sorting into multivesicular endosomes. Curr Opin Cell Biol **15,** 446-455.

Rambourg, A., and Clermont, Y. (1990). Three-dimensional electron microscopy: structure of the Golgi apparatus. Eur J Cell Biol **51,** 189-200.

Renault, L., Guibert, B., and Cherfils, J. (2003). Structural snapshots of the mechanism and inhibition of a guanine nucleotide exchange factor. Nature **426,** 525-530.

Renna, L., Hanton, S.L., Stefano, G., Bortolotti, L., Misra, V., and Brandizzi, F. (2005). Identification and characterization of AtCASP, a plant transmembrane Golgi matrix protein. Plant Mol Biol **58,** 109-122.

Ritzenthaler, C., Nebenfuhr, A., Movafeghi, A., Stussi-Garaud, C., Behnia, L., Pimpl, P., Staehelin, L.A., and Robinson, D.G. (2002). Reevaluation of the effects of brefeldin A on plant cells using tobacco Bright Yellow 2 cells expressing Golgi-targeted green fluorescent protein and COPI antisera. Plant Cell **14,** 237-261.

Rossanese, O.W., Soderholm, J., Bevis, B.J., Sears, I.B., O'Connor, J., Williamson, E.K., and Glick, B.S. (1999). Golgi structure correlates with transitional endoplasmic reticulum organization in Pichia pastoris and Saccharomyces cerevisiae. J Cell Biol **145,** 69-81.

Rutherford, S., and Moore, I. (2002). The Arabidopsis Rab GTPase family: another enigma variation. Curr Opin Plant Biol **5,** 518-528.

Saint-Jore-Dupas, C., Gomord, V., and Paris, N. (2004). Protein localization in the plant Golgi apparatus and the trans-Golgi network. Cell Mol Life Sci **61,** 159-171.

Samaj, J., Read, N.D., Volkmann, D., Menzel, D., and Baluska, F. (2005). The endocytic network in plants. Trends Cell Biol **15,** 425-433.

Samaj, J., Baluska, F., Voigt, B., Schlicht, M., Volkmann, D., and Menzel, D. (2004). Endocytosis, actin cytoskeleton, and signaling. Plant Physiol **135,** 1150-1161.

Sanderfoot, A.A., Kovaleva, V., Bassham, D.C., and Raikhel, N.V. (2001). Interactions between syntaxins identify at least five SNARE complexes within the Golgi/prevacuolar system of the Arabidopsis cell. Mol Biol Cell **12,** 3733-3743.

Sanmartin, M., Ordonez, A., Sohn, E.J., Robert, S., Sanchez-Serrano, J.J., Surpin, M.A., Raikhel, N.V., and Rojo, E. (2007). Divergent functions of VTI12 and VTI11 in trafficking to storage and lytic vacuoles in Arabidopsis. Proc Natl Acad Sci U S A **104,** 3645-3650.

Satiat-Jeunemaitre, B., and Hawes, C. (1992). Redistribution of a Golgi glycoprotein in plant cells treated with Brefeldin A. Journal of Cell Science **103,** 1153-1166.

Seemann, J., Jokitalo, E., Pypaert, M., and Warren, G. (2000). Matrix proteins can generate the higher order architecture of the Golgi apparatus. Nature **407,** 1022-1026.

Serafini, T., Orci, L., Amherdt, M., Brunner, M., Kahn, R.A., and Rothman, J.E. (1991). ADP-ribosylation factor is a subunit of the coat of Golgi-derived COP-coated vesicles: a novel role for a GTP-binding protein. Cell **67,** 239-253.

Shorter, J., and Warren, G. (2002). Golgi architecture and inheritance. Annu Rev Cell Dev Biol **18,** 379-420.

Slusarewicz, P., Nilsson, T., Hui, N., Watson, R., and Warren, G. (1994). Isolation of a matrix that binds medial Golgi enzymes. J Cell Biol **124,** 405-413.

Sohn, E.J., Kim, E.S., Zhao, M., Kim, S.J., Kim, H., Kim, Y.W., Lee, Y.J., Hillmer, S., Sohn, U., Jiang, L., and Hwang, I. (2003). Rha1, an Arabidopsis Rab5 homolog, plays a critical role in the vacuolar trafficking of soluble cargo proteins. Plant Cell **15,** 1057-1070.

Spector, I., Shochet, N.R., Kashman, Y., and Groweiss, A. (1983). Latrunculins: novel marine toxins that disrupt microfilament organization in cultured cells. Science **219,** 493-495.

Sprague, B.L., and McNally, J.G. (2005). FRAP analysis of binding: proper and fitting. Trends Cell Biol **15,** 84-91.

Staehelin, A. (1991). What Is a Plant Cell? A Response. Plant Cell **3,** 553.

Staehelin, L.A. (1997). The plant ER: a dynamic organelle composed of a large number of discrete functional domains. Plant J **11,** 1151-1165.

Staehelin, L.A., and Moore, I. (1995). The Plant Golgi Apparatus: Structure, Functional Organization and Trafficking Mechanisms. Annual Review of Plant Physiology and Plant Molecular Biology **46,** 261-288.

Stefano, G., Renna, L., Chatre, L., Hanton, S.L., Moreau, P., Hawes, C., and Brandizzi, F. (2006). In tobacco leaf epidermal cells, the integrity of protein export from the endoplasmic reticulum and of ER export sites depends on active COPI machinery. Plant J **46,** 95-110.

Stephens, D.J., Lin-Marq, N., Pagano, A., Pepperkok, R., and Paccaud, J.P. (2000). COPI-coated ER-to-Golgi transport complexes segregate from COPII in close proximity to ER exit sites. J Cell Sci **113 (Pt 12),** 2177-2185.

Thompson, J.D., Higgins, D.G., and Gibson, T.J. (1994). CLUSTAL W: improving the sensitivity of progressive multiple sequence alignment through sequence weighting, position-specific gap penalties and weight matrix choice. Nucleic Acids Res **22,** 4673-4680.

Tse, Y.C., Mo, B., Hillmer, S., Zhao, M., Lo, S.W., Robinson, D.G., and Jiang, L. (2004). Identification of multivesicular bodies as prevacuolar compartments in Nicotiana tabacum BY-2 cells. Plant Cell **16,** 672-693.

Ueda, T., Yamaguchi, M., Uchimiya, H., and Nakano, A. (2001). Ara6, a plant-unique novel type Rab GTPase, functions in the endocytic pathway of Arabidopsis thaliana. Embo J **20,** 4730-4741.

Ueda, T., Uemura, T., Sato, M.H., and Nakano, A. (2004). Functional differentiation of endosomes in Arabidopsis cells. Plant J **40,** 783-789.

Uemura, T., Ueda, T., Ohniwa, R.L., Nakano, A., Takeyasu, K., and Sato, M.H. (2004). Systematic analysis of SNARE molecules in Arabidopsis: dissection of the post-Golgi network in plant cells. Cell Struct Funct **29,** 49-65.

Vasudevan, C., Han, W., Tan, Y., Nie, Y., Li, D., Shome, K., Watkins, S.C., Levitan, E.S., and Romero, G. (1998). The distribution and translocation of the G protein ADP-ribosylation factor 1 in live cells is determined by its GTPase activity. J Cell Sci **111 (Pt 9),** 1277-1285.

Vernoud, V., Horton, A.C., Yang, Z., and Nielsen, E. (2003). Analysis of the small GTPase gene superfamily of Arabidopsis. Plant Physiol **131,** 1191-1208.

Vitale, A., and Denecke, J. (1999). The endoplasmic reticulum-gateway of the secretory pathway. Plant Cell **11,** 615-628.

Wang, J., Li, Y., Lo, S.W., Hillmer, S., Sun, S.S., Robinson, D.G., and Jiang, L. (2007). Protein mobilization in germinating mung bean seeds involves vacuolar sorting receptors and multivesicular bodies. Plant Physiol **143,** 1628-1639.

Wennerberg, K., Rossman, K.L., and Der, C.J. (2005). The Ras superfamily at a glance. J Cell Sci **118,** 843-846.

Xu, J., and Scheres, B. (2005). Dissection of Arabidopsis ADP-RIBOSYLATION FACTOR 1 function in epidermal cell polarity. Plant Cell **17,** 525-536.

Zeeh, J.C., Zeghouf, M., Grauffel, C., Guibert, B., Martin, E., Dejaegere, A., and Cherfils, J. (2006). Dual specificity of the interfacial inhibitor brefeldin a for arf proteins and sec7 domains. J Biol Chem **281,** 11805-11814.

Zheng, H., Camacho, L., Wee, E., Batoko, H., Legen, J., Leaver, C.J., Malho, R., Hussey, P.J., and Moore, I. (2005). A Rab-E GTPase mutant acts downstream of the Rab-D subclass in biosynthetic membrane traffic to the plasma membrane in tobacco leaf epidermis. Plant Cell **17,** 2020-2036.

Zhu, Y., Traub, L.M., and Kornfeld, S. (1998). ADP-ribosylation factor 1 transiently activates high-affinity adaptor protein complex AP-1 binding sites on Golgi membranes. Mol Biol Cell **9,** 1323-1337.

PUBLICATIONS

Renna L. *et al*. (to be submitted). Dynamics and distribution of Arf B1b and Arf B1c GTPases in *N. tabacum* plant cells.

Masi E., Ciszak M., Stefano G., **Renna L.**, Azzarello E., Pandolfi C., Mugnai S., Baluska F., Arecchi F.T., Mancuso S. (2009). Spatio-temporal dynamics of the electrical network activity in the root apex. PNAS, in press.

Hanton SL., Chatre L., **Renna L.**, Matheson LA., Brandizzi F.
De novo formation of plant endoplasmic reticulum export sites is membrane cargo induced and signal mediated. Plant Physiol. 2007 Apr;143(4):1640-50.

Matheson LA., Hanton SL., Rossi M., Latijnhouwers M., Stefano G., **Renna L.**, Brandizzi F. Multiple roles of ADP-ribosylation factor 1 in plant cells include spatially regulated recruitment of coatomer and elements of the Golgi matrix.
Plant Physiol. 2007 Apr;143(4):1615-27.

Di Sansebastiano, GP.; **Renna, L.**; Gigante M., De Caroli M., Piro G., Dalessandro G. Green fluorescent protein reveals variability in vacuoles of three plant species (2007) Biologia Plantarum, 51: 49-55

Stefano G., **Renna L.**, Hanton SL., Chatre L., Haas TA., Brandizzi F.
ARL1 plays a role in the binding of the GRIP domain of a peripheral matrix protein to the Golgi apparatus in plant cells. Plant Mol Biol. 2006 Jun;61(3):431-49.

Stefano G, **Renna L**, Chatre L, Hanton SL, Moreau P, Hawes C, Brandizzi F.
In tobacco leaf epidermal cells, the integrity of protein export from the endoplasmic reticulum and of ER export sites depends on active COPI machinery.
Plant J. 2006 Apr;46(1):95-110.

Hanton SL., **Renna L.**, Bortolotti LE., Chatre L., Stefano G., Brandizzi F. Diacidic Motifs Influence the Export of Transmembrane Proteins from the Endoplasmic Reticulum in Plant Cells. Plant Cell. (2005) 17(11): 3081-93

Renna L., Hanton SL., Stefano G., Bortolotti L., Misra V., Brandizzi F. Identification and characterization of AtCASP, a plant transmembrane Golgi matrix protein. Plant Mol Biol (2005) 58: 109-122

Hanton SL., Bortolotti L., **Renna L**., Stefano G., Brandizzi F. Crossing the divide--transport between the endoplasmic reticulum and Golgi apparatus in plants. Traffic (2005) 6: 267-277.

Di Sansebastiano G-P., **Renna L.**, Piro G., Dalessandro G. "Stubborn GFPs in Nicotiana tabacum vacuoles" (2004). Plant Biosystems, 138: 37-42.

International acknowledgments

Citation from **Faculty of 1000 Biology** for the publication: Matheson LA, Hanton SL, Rossi M, Latijnhouwers M, Stefano G, **Renna L**, Brandizzi F. Multiple roles of ADP-ribosylation factor 1 in plant cells include spatially regulated recruitment of coatomer and elements of the Golgi matrix. Plant Physiol. 2007 Apr;143(4):1615-27. Epub 2007 Feb 16. http://www.f1000biology.com/article/id/1085875
"This paper identifies a new effector (GDAP1) for ADP-ribosylation factor..." Evaluated by Faculty of 1000 Biology member **David Oppenheimer** (University of Florida, United States of America)

Abstracts

2002: - Di Sansebastiano G-P, **Renna L,** De Caroli M, Piro G, Dalessandro G: Differenze fra i sistemi vacuolari di *Nicotiana tabacum* e *Arabidopsis thaliana* – 97° Congresso della Società Botanica Italiana. September 2002 - Università degli Studi di Lecce, Italy.

2003: Di Sansebastiano G-P, **Renna L,** Piro G, Dalessandro G: "Stubborn GFPs in *Nicotiana tabacum* vacuoles" S.E.B. SYMPOSIUM: membrane trafficking in plants. August2003- University of Glasgow, UK.

2004: Brandizzi F, Hawes C, Hanton SL, **Renna L**, Stefano G: Use of fluorescent proteins to dissect the dynamics of the plant secretory pathway. European Microscopy Congress 2004, Antwerpen, Belgium. August 2004

2007: Masi E, Ciszak M, Montina A, Malachovska V, Mugnai S, Azzarello E, Pandolfi C, **Renna L**, Stefano G, Voigt B, Hlavacka A, Arecchi FT, Mancuso S.: Spatio-temporal dynamics of the electrical network activity in the root apex. A multi-electrode array (MEA) study. 3rd International Symposium on Plant Neurobiology 14-18 May 2007, Štrbské pleso, SLOVAKIA

2008: Masi E, Ciszak M, Pandolfi C, Azzarello E, Mugnai S, Renna L, **Stefano G**, Voigt B, Mancuso S.: Characteristics of the artificial electrical activity generated in plant roots under artificial changes in gravity. 4rd International Symposium on Plant Neurobiology 6-9 June 2008, Fukuoka, JAPAN.

References

Prof **Stefano Mancuso**
Dipartimento di Ortoflorofrutticoltura
Universita`degli studi di Firenze
Viale delle idée 30
50019 Sesto fiorentino (FI)
Tel 055-457 4063
Email: stefano.mancuso@unifi.it

Dr. **Federica Brandizzi**
Associate Professor
MSU-DOE Plant Research Laboratory,
S-238 Plant Biology
Michigan State University, East Lansing, MI 48824
Tel.: Office 517-353-7872, Lab 517-353-3383
Fax: 517-353 9168
Email: brandizz@msu.edu

Dr. **G-P Di Sansebastiano**
Laboratory of Botany - Di.S.Te.B.A.; University of Lecce, Campus ECOTEKNE
Prov. Lecce-Monteroni 73100 Lecce - Italy
Office: +39 0832 298713
E-Mail: gp.disansebastiano@unile.it

Prof. **M.R. Blatt** FRSE Regius Professor of Botany
Laboratory of Plant Physiology and Biophysics
IBLS - Bower Building, University of Glasgow
Glasgow G12 8QQ UK
Phone (+44-(0)141) 330-4451 / 330-4771
Fax (+44-(0)141) 330-4447
E-mail m.blatt@bio.gla.ac.uk

ACKNOWLEDGEMENTS

I deeply want to thank Prof. Stefano Mancuso for his great contribute, in terms of scientific and human support. I would like also to particularly thank Prof. Frantisek Baluska for his scientific advices.

I want to express my gratefulness to Prof. Dieter Volkmann and Prof. Peter Neumann for their useful suggestion during the writing of this thesis.

I would like to acknowledge my colleagues in the lab: Elisa Azzarello, Marianna Faraco, Andrej Hlavacka, Elisa Masi, Sergio Mugnai, Camilla Pandolfi, Susanna Pollastri, Marika Rossi, and Boris Voigt for their friendship and encouragement during difficult moments, and Giovanni Stefano for helping me all the time. My family and all my friends also deserve particular thanks for they were always close to me, even if physically far. I also thank the Ente Cassa di Risparmio di Firenze for having supported my research and me financially.

DECLARATION

I declare that the work submitted here is result of my own investigation, except where otherwise stated. This work has not been submitted to any other University or Institute towards the partial fulfillment of any degree.

Bonn,

Luciana Renna